

ADSORPTION OF AROMATIC HYDROCARBONS AT GAS-WATER INTERFACE

A Thesis

Submitted to the graduate faculty of the
Louisiana State University
Agricultural and Mechanical College
in partial fulfillment of the
requirements for the degree of
Master of Science in Chemical Engineering

in

The Department of Chemical Engineering

by

Suresh Raja

B.Tech., University of Madras, India, 1998

M.S., Louisiana State University, 2001

December 2003

ACKNOWLEDGEMENTS

I would like to sincerely thank Dr. Valsaraj for his support and guidance through my trying times during this program here. I thank Drs. Thibodeaux and Reible for their valuable and constructive comments on this work and for serving on this thesis committee. Before starting my work here, I had little experience in a laboratory environment. I thank Dr. Ravikrishna for his guidance, help and for teaching me to start up on the lab work. I thank all my fellow graduate students for their friendship and useful discussions, which I shared with them.

I thank the Chemical Engineering staff, Darla Dao and Danny Fontenot for their help at all times. I thank Paul, Fred and Bob at the ChemE shop for their help in building my setup and troubleshooting with equipments. I thank my student workers who worked with me in this part of the project. I thank William Bujanda, Julie Newman, and Vedma Rupnarain.

I thank my mother, brother and sister for being supportive. I will always seek blessings of my father who passed away during the summer of 2002. I dedicate this and all my future works to him.

I thank the United States National Science Foundation for funding this project and also thank the LSU Department of Chemical Engineering.

TABLE OF CONTENTS

ACKNOWLEDGEMENTS	II
LIST OF TABLES	V
LIST OF FIGURES	VI
ABSTRACT	VIII
CHAPTER 1. INTRODUCTION	1
1.1 Introduction	1
1.2 Aromatic Hydrocarbons	1
1.3 Sources of Polycyclic Aromatic Hydrocarbons	3
1.4 Organic Compounds in Aerosols and Cloud and Fog Water	5
1.5 Objective of the Study	5
CHAPTER 2. THERMODYNAMICS AND ANALYSIS OF CHEMICALS AT ENVIRONMENTAL INTERFACES	7
2.1 Transport and Fate of Chemical Species	7
2.2 Dry Deposition Pathway	7
2.3 Wet Deposition Pathway	7
2.4 Henry's Law Equilibrium	8
2.5 Hydrophobicity and its Importance at a Gas-Water Interface	9
2.5 Thermodynamics of Air-Water Interface	10
2.6 "Critical Cluster" Model – (a gas-to-liquid transport model)	13
2.7 Measurement of Adsorption	14
2.7.1 Drop-Weight Method	15
2.7.2 Wilhelmy Plate Method	16
CHAPTER 3. THEORY OF INVERSE GAS CHROMATOGRAPHY	18
3.1 Introduction	18
3.2 Adsorption-Dissolution in Inverse Gas Chromatography	18
3.3 Physical Insight of K_{IA}	20
3.4 Retention Volumes	20
3.5 Gibbs-Helmholtz Equation	21
3.6 Gas-Solid Interface	26
3.7 Theory of Adsorption	26
3.8 Adsorption on Dry Diatomaceous Earth	27
CHAPTER 4. EXPERIMENTAL METHODOLOGY	28
4.1 Sample Probe Gas Preparation	28
4.1.1 Benzene Vapor Probe Preparation	28
4.1.2 Naphthalene and Phenanthrene Vapor Probe Preparation	29
4.2 Schematics of the IGC Experiment	30

4.3 Detection System	31
4.4 Gas Chromatographic Columns	33
4.4.1 Water Coated Column Preparation	33
CHAPTER 5. RESULTS AND DISCUSSION.....	34
5.1 Adsorption of Organic Compounds on Gas-Solid Interface.....	34
5.2 Adsorption of Benzene at Gas-Solid Interface	35
5.3 Adsorption of Naphthalene at Gas-Solid Interface.....	36
5.4 Adsorption of Phenanthrene at Gas-Solid Interface	38
5.5 Analysis of Gas-Solid Adsorption Results	39
5.6 Adsorption of Organic Compounds at Gas-Water Interface.....	41
5.6.1 Determination of Specific Surface Area of Water Loaded Column Packing.....	41
5.7 Adsorption of Benzene in Gas-Water interface	42
5.8 Adsorption of Naphthalene at the Gas-Water Interface.....	46
5.9 Adsorption of Phenanthrene at the Gas-Water Interface	48
5.10 Analysis of Gas-Water Interface Adsorption Results.....	51
5.10.1 Influence of Adsorbent Surface Morphology on Adsorbate Binding.....	53
5.10.2 Analysis of Interfacial Adsorption via Cluster Formation.....	54
5.11 Correlation of K_{IA} and P_{SL}^0 for Aromatic Hydrocarbons	56
CHAPTER 6. APPLICATIONS IN ATMOSPHERIC CHEMISTRY	58
6.1 Introduction.....	58
6.2 Enrichment of Organic Vapors in Fog Water	58
6.3 Transport of Gaseous Species into Fog Droplet	59
CHAPTER 7. CONCLUSIONS AND FUTURE WORK	63
7.1 Conclusions.....	63
7.2 Future Work.....	63
REFERENCES.....	64
VITA	72

LIST OF TABLES

TABLE 1. PHYSICOCHEMICAL PROPERTIES OF THE AROMATIC HYDROCARBONS [VALSARAJ, 2000, CABANI ET AL, 1981].....	4
TABLE 2. PHENANTHRENE GAS-SOLID ADSORPTION EXPERIMENTS.....	39
TABLE 3. GAS-SOLID ADSORPTION THERMODYNAMICS OF AROMATIC HYDROCARBONS....	40
TABLE 4. BENZENE PARTITION CONSTANT AS FUNCTION OF TEMPERATURE.	44
TABLE 5. NAPHTHALENE PARTITION CONSTANT AS FUNCTION OF TEMPERATURE.	47
TABLE 6. PHENANTHRENE PARTITION CONSTANT AS FUNCTION OF TEMPERATURE.....	50
TABLE 7. PARAMETERS FOR ADSORPTION AT GAS-SOLID AND GAS-WATER INTERFACE	52
TABLE 8. HENRY'S CONSTANT AND K_{IA} OF BENZENE, NAPHTHALENE AND PHENANTHRENE	60

LIST OF FIGURES

FIGURE 1. MOLECULAR STRUCTURE OF POLYCYCLIC AROMATIC HYDROCARBONS (PAHs)	2
FIGURE 2. ILLUSTRATION OF GAS-LIQUID PARTITIONING	12
FIGURE 3. ILLUSTRATION OF GIBBS LAW TO OBTAIN SURFACE ADSORPTION CONSTANT (SURFACE TENSION, Γ VERSUS CONCENTRATION, C).	14
FIGURE 4. DROP-WEIGHT OR DROP-VOLUME METHOD FOR SURFACE TENSION MEASUREMENT.	15
FIGURE 5. WILHELMY-PLATE METHOD FOR SURFACE TENSION MEASUREMENT.	16
FIGURE 6. ADSORPTION-DISSOLUTION IN INVERSE GAS CHROMATOGRAPHY.....	19
FIGURE 7 PREPARATION OF ORGANIC VAPORS FROM FLASKS MAINTAINED IN TEMPERATURE CONTROLLED OVENS.	28
FIGURE 8. SCHEMATICS OF THE GAS-WATER INTERFACE ADSORPTION EXPERIMENT.	31
FIGURE 9. FLAME IONIZATION DETECTOR.....	32
FIGURE 10. HEAT OF ADSORPTION OF BENZENE ON A GAS-SOLID INTERFACE ($R^2=0.9932$).	35
FIGURE 11. HEAT OF ADSORPTION OF NAPHTHALENE ON A GAS-SOLID INTERFACE ($R^2=0.8075$).....	37
FIGURE 12. HEAT OF ADSORPTION OF PHENANTHRENE ON A GAS-SOLID INTERFACE ($R^2=0.9993$).....	38
FIGURE 13. ESTIMATION OF SPECIFIC SURFACE AREA OF WATER LOADED PACKING ($R^2=0.912$).....	42
FIGURE 14. PLOT OF V_N/V_W VERSUS A_W/V_W FOR BENZENE AT 298 K ($R^2 = 0.996$)	43
FIGURE 15. INTEGRAL FORM OF THE GIBBS-HELMHOLTZ EQUATION FOR BENZENE ($R^2=0.998$).....	44
FIGURE 16. BENZENE VAPOR INJECTION VOLUMES 25 ML TO 100 ML (WATER LOADING= 0.32 G/G, 298 K).....	45
FIGURE 17. PLOT OF V_N/V_W VERSUS A_W/V_W FOR NAPHTHALENE AT 298 K ($R^2 = 0.992$).	46

FIGURE 18. INTEGRAL FORM OF THE GIBBS-HELMHOLTZ EQUATION FOR NAPHTHALENE ($R^2=0.936$).....	47
FIGURE 19. PLOT OF V_N/V_W VERSUS A_W/V_W FOR PHENANTHRENE AT 363 K ($R^2 = 0.99$).	49
FIGURE 20. INTEGRAL FORM OF THE GIBBS-HELMHOLTZ EQUATION FOR PHENANTHRENE ($R^2=0.892$).....	50
FIGURE 21. CRITICAL CLUSTER SIZE FOR AROMATIC HYDROCARBONS FROM THERMODYNAMIC PARAMETERS.	54
FIGURE 22. CORRELATION OF $\log(K_{IA})$ AND $\log(P_{SL}^0)$ FOR AROMATIC HYDROCARBONS. DATA FROM THIS WORK AND PANKOW, 1997. ($R^2=0.9797$).	57
FIGURE 23. NORMALIZED DEVIATION IN HENRY'S LAW VERSUS DROPLET SIZE IN MICRONS (SOLID LINE - NAPHTHALENE AND POINTS – BENZENE)	61
FIGURE 24. NORMALIZED DEVIATION IN HENRY'S LAW VERSUS DROPLET SIZE IN MICRONS. (PHENANTHRENE)	61

ABSTRACT

Adsorption of organic vapors at a gas-water interface has several physical applications with respect to natural processes in the environment. Understanding the adsorption processes is critical in development of risk assessment and modeling of transport and fate of various chemical species that are abundantly present in the environment. Evidences from the works of several researchers point out deviations in gas-liquid partitioning as predicted by Henry's law. In view of several theories that describe these deviations, adsorption process is hypothesized to be significant in gas-liquid partitioning, in addition to temperature and presence of organic matter, particularly on liquid surfaces with high surface to volume ratio. Implications of these adsorption and thermodynamic parameters of chemical species have been applied to its atmospheric fate and transport.

In this work, inverse gas chromatography has been used to determine surface adsorption partition constant for organic compounds such as benzene, naphthalene and phenanthrene. A water-coated diatomaceous earth was used as the packing support material in the chromatographic column. The probe used to study this gas-liquid partitioning was obtained in vapor phase and injected in the chromatograph with dry support material and water coated support. The retention volume on the water-coated support, depends on two processes, the adsorption and dissolution process in the liquid coated surface, and was primarily used to extract the partition constants. The Gibbs-Helmholtz equation was used to determine the enthalpy of adsorption.

The enthalpy of adsorption indicates that the adsorption process is more favorable at the gas-solid interface than at the gas-water interface, supporting the surface

morphology theory based on fractal dimensions. The enthalpy of adsorption at the gas-water interface for all three compounds was larger than the enthalpy of condensation and the enthalpy of aqueous solvation. This supports the prevailing “critical cluster” model for the dynamics of the transfer of compounds from the gas-water interface. The partition constant at the gas-water interface was correlated with the sub-cooled liquid vapor pressure of the PAHs along with data obtained from other works. Partition constants indicate that the most hydrophobic compound will experience enhanced surface adsorption and hence scavenged the most by wet deposition process.

CHAPTER 1

INTRODUCTION

1.1 Introduction

There is an abundance of natural environmental processes where in gas phase molecules interact with liquids; essentially water. Along with these natural processes there are several industrial processes that utilize gas-liquid interactions, such as distillation and desiccation. The interface between the gas and liquid becomes largely important in view of partitioning of species between the two phases. In the case of hydrophobic compounds the interface acts as a sink to accumulate these chemical species. Usually, the Henry's Law gives the partitioning of gas phase species in the bulk liquid and gas. However, interface adsorption can effect the prediction of gas-liquid partitioning.

1.2 Aromatic Hydrocarbons

There are several organic compounds that are present in the atmosphere but most do not form aerosols under atmospheric conditions due to their high vapor pressure. But there are a class of organic compounds namely Poly Aromatic Hydrocarbons (PAH) that are unlikely to form aerosols and are present in the gas phase. They are hydrophobic, low vapor pressure compounds present in the gas phase that are scavenged by deposition. Gas-aerosol partitioning and aerosol transport have been of interest in atmospheric sciences, and Fuchs has dealt the aerosol dynamics extensively in his classical work ([Fuchs, 1964](#)). Simulation methodologies for aerosol transport have been of interest here at LSU ([Sajo and Raja 2002](#), [Raja, 2001](#)) and to several other researchers elsewhere ([Reynolds et al, 1974](#), [McFarland et al, 1997](#), [Karditsas et al, 2002](#)).

The vapor pressures of PAHs vary over seven orders of magnitude. As a result, certain compounds in this class are present exclusively in the gas phase while the others are present in the aerosol phase or both gas and aerosol phases.

In this work three compounds have been chosen to study the gas-liquid partitioning namely, benzene, naphthalene and phenanthrene. The rationale in choosing these compounds can be attributed to their existence exclusively in the gas phase, at 25 °C, due to low gas-aerosol partition constant ($C_{\text{aer}}/C_{\text{g}}$) in the order of 10^{-2} to 10^{-3} , while the other compounds in this class, such as Benzo[a]pyrene and Chrysene, are present predominantly present in the aerosol phase with higher $C_{\text{aer}}/C_{\text{g}}$ ([Pankow and Bidleman, 1991](#)). Also, it has been identified that this class of compounds are ubiquitous ([Saxena, P., Hildemann 1996, L. M., Baek et al, 1991](#)) and are identified in the form of bicyclic gas-phase naphthalene to seven or more fused ring species such as coronene.

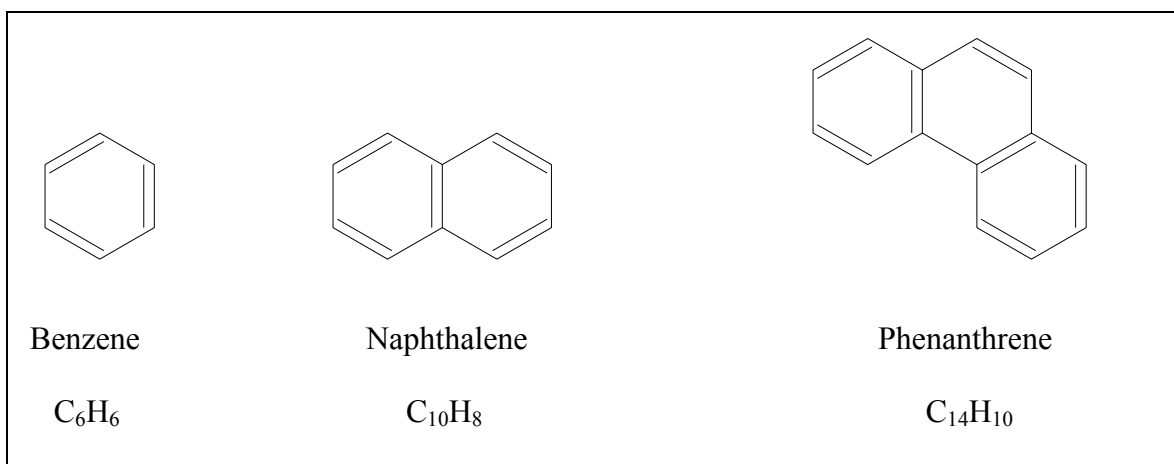


Figure 1. Molecular Structure of Polycyclic Aromatic Hydrocarbons (PAHs)

1.3 Sources of Polycyclic Aromatic Hydrocarbons

Most of the sources of PAHs are anthropogenic, formed during the incomplete combustion of organic matter such as coal, oil, gasoline fuel and wood ([Jenkins et al, 1996](#)). While other sources of PAHs are natural forest fires and volcanic eruptions ([Nikolaou et al, 1984](#)). Sources such as residential heating, industrial processes, open burning, and power generation are estimated to account for roughly 80% of the annual total PAH emissions in the United States with the remainder produced by automobile sources ([Peters et al, 1981](#), [Ramdahl et al, 1984](#)).

The presence of PAHs in water, aquatic sediments and organisms has been recognized for more than 40 years ([Neff, 1979](#)). With the development of sensitive high-resolution techniques for the analysis of PAH in environmental samples, it has become apparent that extremely complex mixtures of PAHs, including the carcinogenic forms of benzo[a]pyrene, are nearly ubiquitous trace contaminants of aquatic ecosystems. A considerable amount of research has been conducted in recent years on the sources, fates and biological effects of these PAH mixtures in aquatic ecosystems by [Andelman and Suess, 1970](#) and [Andelman and Snodgrass, 1972](#). The sources of PAH found in these aquatic systems are myriad ranging from endogenous to anthropogenic. However, the endogenous sources of PAHs are static and remain in the organism and ecosystem. The anthropogenic sources of PAH reach the aquatic environment by spillage of crude and refined oil, in industrial and domestic effluents, runoff water from land, and by dry or wet deposition in the atmosphere. Hence, it is important to understand the fate and transport dynamics of PAH in the environment.

A twelve-month monitoring program for PAHs and carbonyl compounds were performed in Hong Kong ([S.C.Lee et al, 2001](#)). Their studies show highest concentration of Naphthalene ($=993 \text{ ng/m}^3$) and high concentrations of other PAHs, such as phenanthrene, anthracene, and pyrene, in the urban atmosphere of Hong Kong among the other PAHs. Similar studies on PAHs show their presence in Munich ([Schnelle-Kreis et al, 2000](#)). Also, studies done here in metro Baton Rouge area by [Subramanyam et al, 1994](#) characterize their presence in the air.

TABLE 1. PHYSICOCHEMICAL PROPERTIES OF THE AROMATIC HYDROCARBONS [[VALSARAJ, 2000](#), [CABANI ET AL, 1981](#)]

Property	Benzene	Naphthalene	Phenanthrene
Molecular weight	78	128	178
Solubility in Water [$\mu\text{g/mL}$]	170	31.7	1.29
Sub cooled liquid vapor pressure, $P_s(l)^\circ$ [kPa]	12.7	0.037	9×10^{-5}
Enthalpy of condensation, ΔH° [kJ/mol]	-34	-58	-75
Enthalpy of solvation, $\Delta_{\text{solv}}H^\circ$ [kJ/mol]	-31	-47	-54

Table 1 lists the physicochemical properties of aromatic hydrocarbons that were used in this study. Each of these compounds (benzene, naphthalene and phenanthrene) is hydrophobic. The decreasing aqueous solubility and vapor pressure with increase in molecular weight indicate increasing hydrophobic nature of the molecules. Of the three

compounds listed, the last two compounds are an important class of compounds known as Polycyclic Aromatic Hydrocarbons (PAHs) that are ubiquitous in air and due to its hydrophobic nature accumulate in organic rich environments such as lipids, aerosols and soil particles.

With only carbon and hydrogen, PAHs are very stable organic molecules. These molecules are flat, with each carbon having three neighboring atoms much like graphite. Some of the compounds under this class of PAHs are suspected carcinogens and hence their fate and transport in environment is of much interest. The first few studies with respect to the carcinogenic nature of these PAHs were by [Bingham et al, 1979](#). Most of the studies reported by Bingham were of the occurrences of cancer among workers in refinery workers. More recently, [Lewis et al, 1984](#) showed carcinogenic potential of petroleum hydrocarbons on skin.

1.4 Organic Compounds in Aerosols and Cloud and Fog Water

A significant part of atmospheric aerosols and cloud droplets, upto 70%, consist of organic compounds ([Saxena and Hildemann, 1996](#), [Zappoli et al, 1999](#), [Facchini et al, 1999](#)). Many researchers around the world have also shown unexpectedly high concentrations of pesticides and also hydrophobic compounds in fog waters ([Glotfelty et al, 1987](#), [Schomburg et al, 1991](#), [Capel et al, 1990](#)). Fog-water sampling in various parts of the world shows presence of various organic compounds ([Zhang and Anastasio 2001](#), [Glotfelty 1990](#)).

1.5 Objective of the Study

Currently there are no experimental data on the adsorption of benzene, naphthalene and phenanthrene at the gas-water interfaces. Having the adsorption and

thermodynamic parameters of these compounds, can lead to better prediction of their enrichment at various environmental interfaces, such as cloud water and fog water. In this work, the various thermodynamic and adsorption parameters are determined by inverse gas chromatography and a correlation of the partition constant is obtained for various PAHs. Implications of this work with regards to atmospheric chemistry are to be elucidated.

CHAPTER 2

THERMODYNAMICS AND ANALYSIS OF CHEMICALS AT ENVIRONMENTAL INTERFACES

2.1 Transport and Fate of Chemical Species

The fate and transport of a chemical species is broadly subject to two paths of removal from the atmosphere, namely the dry and wet deposition. The method of scavenging (deposition) and the resulting partitioning of a chemical species depend on the various properties of the species in question, atmospheric conditions, and the surface topography.

2.2 Dry Deposition Pathway

Based on the gas-aerosol partition constant, mentioned earlier, the chemical species are present in the gaseous or particulate (aerosol) form, and this in turn determines the path of deposition process. The fundamental aspect of dry deposition includes transport of gaseous and particulate matter from the atmosphere onto the natural ground surfaces in the absence of precipitation. The nature of the surface itself is a factor in a dry deposition process. Natural surfaces, such as vegetation, generally promote dry deposition ([Seinfeld and Pandis, 1998](#)).

2.3 Wet Deposition Pathway

Wet removal pathways involve a number of phases and depend on multiple processes. Wet deposition involves transfer of soluble gas or a particle into rain droplet, cloud or fog water. The rate of transfer of the air, which may comprise both gas and particles into aqueous phase, is defined by the term called washout ratio ([Eisenreich et al, 1981](#)),

$$W = \frac{C_{aq}}{C_{air}}, \quad (1)$$

Where C_{aq} and C_{air} are the total concentrations of the chemicals in the aqueous phase and air. The wet deposition is relatively complex in comparison to the dry deposition process, primarily due to the involvement of multiple phases. The multiple phases include the three phases, gas, aerosol, and aqueous. In addition, the possibility of the presence of aqueous phase in several other forms, such as fog-water, rain, snow, ice crystals, sleet, and hail, complicates the process even further.

The importance of gas and particle scavenging can be highlighted by the following equation ([Van Ry et al, 2002](#)), $W_T = W_G \cdot (1 - \varphi) + W_P(\varphi)$, where W_G and W_P is the gas phase and particle phase scavenging coefficients, respectively, and φ is the fraction present as atmospheric particles. W_G is the inverse of the compound's Henry's Law Constant.

2.4 Henry's Law Equilibrium

Usually, the partitioning of a chemical species between the gas and a condensed phase (water) is calculated assuming equilibrium between the phases and is given by Henry's Law ([Schwartz 1983](#), [Seinfeld 1986](#)). Consider a soluble species that exists around a foggy atmosphere or falling raindrops. The rate of transfer of a gas to the surface of a stationary or falling drop (W_i) can be calculated by

$$W_i = K_C (C_g - C_{eq})$$

$$H = \frac{C_{aq}}{C_{eq}} \quad (2)$$

Most of the transport models use only dissolution for calculating the wet deposition fluxes. The model of atmospheric transport and chemistry, known as MATCH,

considers only dissolution of species in the liquid phase is taken into account, hence given by Henry's Law ([Crutzen and Lawrence, 2000](#)).

In most of the atmospheric studies, where both the gas and the bulk aqueous phase concentrations has been measured, significant deviations in Henry's law has been observed ([Richards et al 1983](#), [Munger et al 1990](#), [Winiwarter et al 1988](#)). This deviation can be particularly consequential in the case of cloud-water and fog-water samples.

[Pandis and Seinfeld, 1991](#) have been put forward theories to explain this "Henry's Law Deviations". Work by ([Karger et al, 1971](#)), ([Valsaraj, 1988](#)) and ([Mackay et al, 1991](#)) have postulated and evidenced the air-water interface to be a significant compartment for species accumulation in this regard. More recently ([Hoff et al, 1993](#)) have discussed evidence in support of their contentions.

Species accumulation at the interface can be considerable; in the case of hydrophobic compounds accumulation at the interface is significant. The hydrophobic nature of a chemical species is attributed to their chemical property, such as low aqueous solubility. From Table 1, the compounds analyzed in this work are hydrophobic, and have low vapor pressure and aqueous solubility.

2.5 Hydrophobicity and its Importance at a Gas-Water Interface

The "solvophobic theory" proposed by ([Franks and Evans, 1945](#)) describes a large decrease in entropy upon dissolution of non-polar compounds in water, due to increased ordering of water molecules around the non-polar molecule. Recently, [Dang and Feller, 2000](#) has shown the existence of this free energy minimum, in a benzene-water system, at the interface as shown in Figure 2. Further, ([Eley, 1939](#)) this free energy has two components (1) that forms a cavity in the bulk water to accommodate the solute and (2)

solute-water interactions. The cavity formation energy is the principal component that arises from the re-structuring of the water molecules around the non-polar molecule. In the case of Benzene-Water system, [Dang and Feller, 2000](#) have shown that the benzene molecule lies parallel to the dividing surface.

Physically speaking, when a hydrophobic solute is in an aqueous solution, the unfavorable interaction between solute and solvent can lead to the solute adjusting its configuration to minimize its solvent exposed area. To quantify these theories several simulations and theoretical studies have been done ([Weeks et al 1998](#), [Floris et al, 1997](#)). [Lum, Chandler and Weeks, 1999](#) have shown the formation of a vapor layer in the immediate vicinity of the solute in the case of larger solute molecules. The introduction of the solute molecule tends to replace the strong hydrogen bonds between water molecules with the weaker solute-water intermolecular forces. Those molecules that cannot compete with hydrogen bonds between water molecules are squeezed out of the interstices of the water structure. These molecules that are squeezed out to minimize the structure disruption, as also cavitation energy is unfavorable (no bubbles), prefer a compartment “the air-water interface” where least number of water molecules interact with them. Thus, interface is important and act as zone for accumulation of a species, and is particularly important in the case of a hydrophobic solute.

2.5 Thermodynamics of Air-Water Interface

Figure 2 shows a free energy minimum at the air-water interface during an adsorption process. This energy barrier inhibits desorption and dissolution of hydrophobic compounds, and tends to concentrate the chemical species at the interface. The eventual dissolution of the chemical species depends on the size cluster of molecules

formed at the interface, explained in section 2.6. Higher this free energy minimum/barrier, higher the cluster size required for subsequent dissolution. This energy barrier, oppose both removal of polar hydroxyl group from water and the immersion of hydrocarbon in the chemical species in water, which as a result, squeezes the species out to the interface. Also, it is imperative to note that the transport of chemical species to the interface is governed by diffusion alone. The nature of the chemical species to be more non-polar (hydrophobic) increases the tendency of the adsorbing species to accumulate at the interface. Thus, the amount of chemical species that accumulates at the interface increase till the chemical potential of the surface and the bulk are equal. Thus, resulting in greater concentration of solute in the surface than at the bulk, adding significance to the gas-water interface as an enrichment zone.

$$\mu_o + RT \ln (c) = \mu_i^o + RT \ln (c_s) \quad (3)$$

In the above equation, μ is the chemical potential of the solute in solution, superscript “o” denotes that the chemical potential refers to standard state, and subscript refers to material in the surface. The terms c and c_i refer to bulk and interface-surface concentration. At equilibrium the surface concentration builds up to the level where $\mu = \mu_i$ and,

$$\frac{c_s}{c} = \exp \left[\frac{(\mu^o - \mu_i^o)}{RT} \right] = \exp \left[\frac{\lambda}{RT} \right] \quad (4)$$

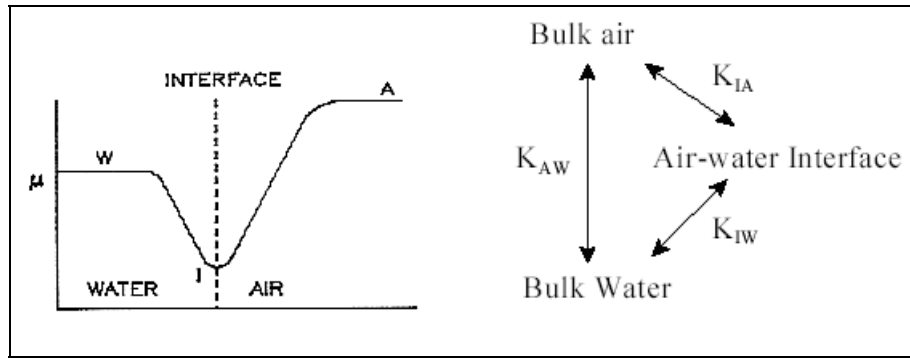


Figure 2. Illustration of gas-liquid partitioning

[Dang and Feller, 2000](#) simulated a free energy profile for benzene-water system by molecular dynamics. The free energy minimum for the benzene-water system was -4 kcal/mole. The existence of this large free energy minimum, shown in Figure 2, is an indication that the benzene molecule is surface active. The calculated adsorption free energy from their simulation is about -4 kcal/mol. There were no experimental data, prior to this work, to validate the simulation results of Dang and Feller for the adsorption free energies of the compounds benzene.

The quantity c and c_s in equation (3) and (4) are expressed in units of concentration ($\mu\text{g/mL}$). Due to the existence of this free energy minimum at the interface, $\mu > \mu_i$ in equation (4) and as a result the interface-surface concentration of the chemical species c_i , is greater than the bulk concentration. Thus, it can be hypothesized that the significant deviations in the Henry's from the analysis of the fog-water samples and cloud-water can be attributed to the interface adsorption phenomena. Suitable accommodations for the interface adsorption can predict the actual enrichment/scavenging of solute species in the gas-water partitioning process.

2.6 “Critical Cluster” Model – (a gas-to-liquid transport model)

Now we know the mechanism of hydrophobicity at a gas-water interface and adsorption processes, the mechanism of dissolution into the bulk phase are next in line. The dynamics of the entry of gas molecules at the interface between the gaseous and aqueous phase are evidenced on the basis of “critical cluster” model proposed by [Nathanson et al, 1996](#). The interface is a dynamic region where aggregates are formed via accumulation. The aggregates are formed when the gas phase species are interconnected or bound to the aqueous phase by various configurations and aggregations. Some molecules may be weakly bound and others may be tightly bound hence forming aggregates. The nucleation theory describes that the formation of a new phase is the most viable description of such surface dynamics. Such new phases can be imagined to be in some form of clusters or aggregates that are loosely bound surface species. The critical cluster consists of a specific number of molecules say N that comprise the gas molecules and the water molecules required to form the critical cluster. The number of molecules required to form the critical cluster depend on the structure of the specific molecule undergoing the adsorption process.

The critical cluster model can be summarized as a three-step model as follows, Adsorption \rightarrow Cluster Formation \rightarrow Solvation. Essentially, the ease with which a molecule can be incorporated into the bulk water depends on its ability to enter the nucleation or aggregation process with water molecules at the interface. Once the critical cluster is formed around the molecule, the cluster continues to grow and the whole molecule is enveloped independent of size.

2.7 Measurement of Adsorption

There are several methods available for studying the thermodynamics and kinetics of adsorption and desorption vapors at gas-liquid interface. The lowering of surface tension (γ) can be readily measured by using the Wilhelmy plate method or the drop weight method. Thermodynamically, the surface tension is the free energy per unit area. The overall increase in free energy of the system is the work done in increasing the surface area,

$$\gamma = \left(\frac{\partial G}{\partial A_s} \right) \quad (5)$$

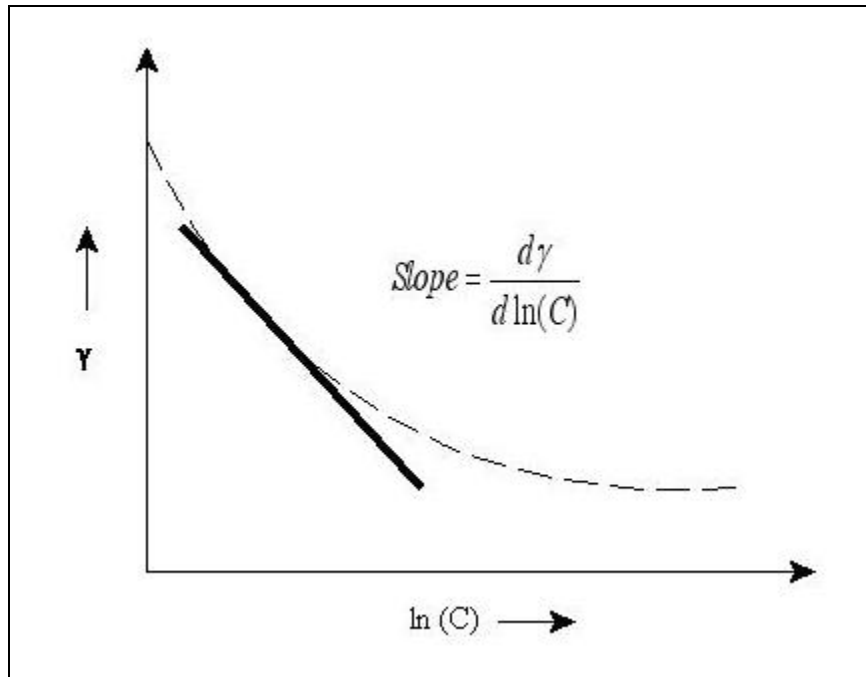


Figure 3. Illustration of gibbs law to obtain surface adsorption constant (surface tension, γ versus concentration, C).

$$\Gamma_i \left(\frac{\text{mol}}{\text{cm}^2} \right) = -\frac{1}{RT} \left(\frac{d\gamma}{d \ln C} \right) \quad (6)$$

Using these surface tension measurements, a plot of surface tension, γ versus the concentration, C , will yield a slope that is the surface concentration Γ_i , and the suffix i represents solute.

2.7.1 Drop-Weight Method

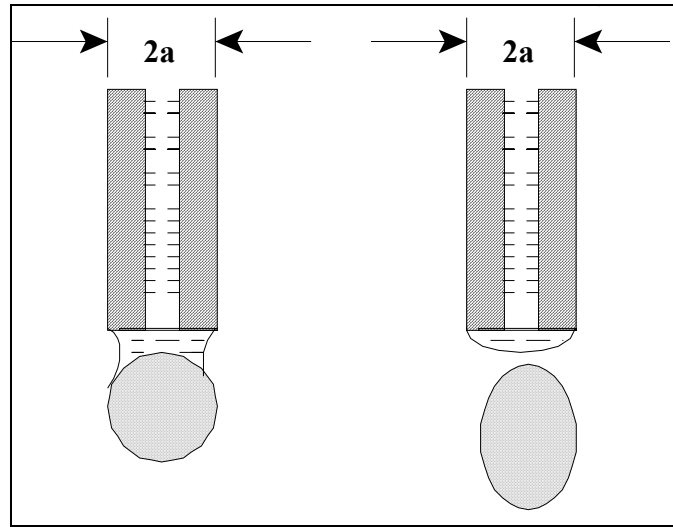


Figure 4. Drop-weight or drop-volume method for surface tension measurement.

The weight (or volume) of each liquid drop, which detaches itself from the tip of a vertical tube, is determined largely by the surface tension of the liquid. Assuming that the drops are formed extremely slowly, they detach themselves completely from the tip, as shown in the Figure 4, when the gravitational pull reaches the restraining force of surface tension.

$$Mg = V\rho_l g = 2\pi a\gamma \quad (7)$$

Where, g is the gravitational acceleration, M and V are the mass and volume of each drop that falls from the tip, ρ_l is the density of the liquid, and a is the radius of the tip of the tube. Solving for γ , the surface tension we have,

$$\gamma = \frac{Mg}{2\pi a} = \frac{V\rho_l g}{2\pi a} \quad (8)$$

However, there are certain correction factors required because the liquid forming the drop does not completely leave the tip of the tube. These correction factors are known from the works of [Harkins and Brown, 1919](#).

2.7.2 Wilhelmy Plate Method

In this method ([Wilhelmy, 1863](#)) a plate is suspended from a beam attached to a torsion wire in a bath containing the liquid to be measured for surface tension. The additional pull on the plate when it becomes partly immersed is equal to the product of the perimeter and the surface tension.

$$\gamma \cos(\theta) = \frac{W_{TOTAL} - (W_{PLATE} - b)}{2l} \quad (9)$$

In the above equation, γ is the surface tension; θ is the contact angle; W_{TOTAL} is the total weight of the bath, contents and the plate, W_{PLATE} is the weight of the plate, b is the buoyancy force, and l is the length of the plate. The numerator in equation (9) is essentially the change in weight of (force exerted by) the plate when brought in contact with the liquid.

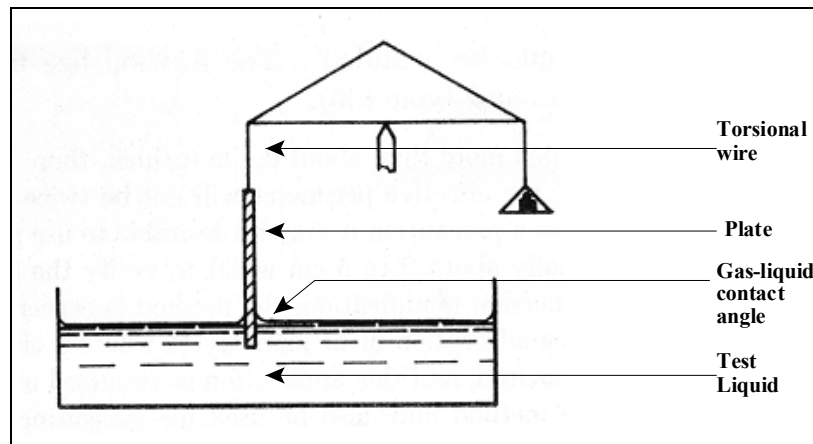


Figure 5. Wilhelmy-plate method for surface tension measurement.

Nevertheless, these static surface measurement techniques are limited to compounds with high vapor pressure. [Dove et al, 1996](#) have shown that to determine surface properties, inverse-gas chromatography technique is more promising than the surface pressure measurement techniques. Several techniques exist to measure the surface energy, for example, sessile drop, and dynamic contact angle measurements. [Grimsey et al, 2002](#), has shown inverse gas chromatography to be an alternative technique to determine thermodynamic parameters.

CHAPTER 3

THEORY OF INVERSE GAS CHROMATOGRAPHY

3.1 Introduction

Generally, in gas chromatography, the sample is vaporized and injected onto the head of a chromatographic column. Elution is brought about by the flow of an inert gaseous mobile phase. In general, the principles of gas chromatography apply to inverse gas chromatography. A brief introduction to the methodology of the IGC is presented in this chapter, and is devoted to the theory and development of basic relations of the IGC technique, and extraction of thermodynamic parameters.

3.2 Adsorption-Dissolution in Inverse Gas Chromatography

Gas Chromatography has been a routine tool for the measurement of thermodynamic parameters of solution ([Cruickshank et al, 1965](#)) and for gas-solid adsorption studies ([Kiselev et al, 1969](#)). Recently, Inverse Gas Chromatography (IGC), a gas phase technique, has found increasing use both in pharmaceutical ([Domingue et al, 2003](#), [York et al, 1998](#)) and chemical thermodynamic analysis ([Karger et al, 1971](#), [Hoff et al, 1993](#)) for characterizing surface and bulk properties of solid materials.

In this method, the mobile phase (gas) is used to introduce probes of known characteristics, and the output, which is the retention time and peak shape, is used to obtain information about the stationary phase. The figure below illustrates the processes involved in IGC. The solid support material is coated with known mass of liquid per gram of the dry support material.

Due to the recent sophistication of the pharmaceutical materials, the need for more sensitive, thermodynamic-based IGC technique has been used to measure process

related changes in surface and bulk properties of materials ([Domingue et al, 2003](#), [Grimsey et al, 2002](#), [York et al, 1998](#)). In this regard, IGC has been known to be a highly sensitive and versatile gas phase technique that is capable of differentiating subtle changes by introducing a wide range of molecular probes (vapor or gas) either at very low concentrations (infinite dilution regime) or at higher concentrations (finite dilution regime) to obtain a comprehensive understanding of both the surface and bulk properties of a material that is used as a support material in the packed column installed in the GC.

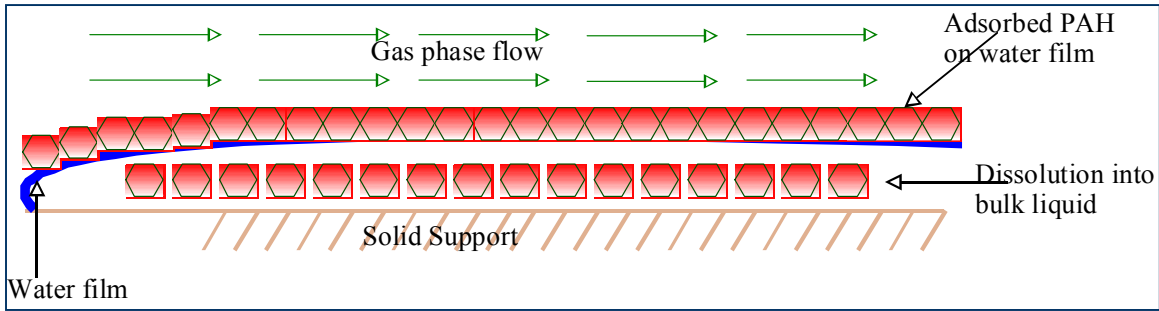


Figure 6. Adsorption-dissolution in inverse gas chromatography.

The carrier gas transports the probe across the coated support material as shown in Figure. The probe molecule gets adsorbed on the water film and also gets dissolved into the bulk liquid. The overall retention time of the probe is due to bulk phase partitioning into the water film as well as the adsorption on the gas-water interface of the water film. The net retention volume per gram of adsorbent is given by

$$V_N (cm^3 / g) = K_{IA} A_W + K_{WA} V_W \quad (10)$$

Where, V_N , A_W and V_W are the total retention time volume, specific gas-water interface area, and volume of water per unit mass of adsorbent. K_{IA} is the gas-water interfacial partition constant and is given as follows,

$$K_{IA} (\mu m) = \frac{\Gamma_i (mol / cm^2)}{C_a (mol / cm^3)} \quad (11)$$

If we assign an area A (m^2) to the interface and then express the concentration on the interface on a mole per unit area basis expressed as Γ_i (mol/m^2), then the partition coefficient K_{IA} is the equilibrium concentration ratio at the interface and the bulk air with units of length. The physical significance of this K_{IA} with units of length is the depth of the bulk gas phase that contains the same amount (moles) of chemical per unit area of as the interface. Hence, we can say that an area of $1\text{m}^2 \times K_{IA} \times C_w$ (moles) contains the same amount as in a volume of the bulk air of 1m^2 in area by K_{IA} (m) deep.

3.3 Physical Insight of K_{IA}

An important consequence of the interfacial adsorption can be of environmental relevance. Consider, a small air bubble rising through a column of water containing dissolved chemical species, for which the equilibrium amount at the interface will be comparable to that in the air phase if K_{IA} is comparable to the bubble diameter. That is, if K_{IA} is in the micron range we can expect high surface adsorption if the bubble size is also in the micron size range. Theoretically, we see that we can achieve enhanced stripping of the dissolved chemical beyond the expected stripping/enrichment predicted by Henry's law. Thus, this is evidently a foresight for us to believe the existence of Henry's law deviation with respect to bubble size. However, it remains a hypothesis in this manuscript at this point to show the dependence of enrichment with droplet size and deviation of Henry's law.

3.4 Retention Volumes

As in any gas chromatographic applications, the retention volume is also fundamental to the methodology of inverse gas chromatography. This retention volume, V_N is the fundamental data from which most of the properties of Gas-Water interface can

be obtained ([Karger et al, 1971](#), [Hartkopf and Karger, 1973](#)). The retention volume V_N is calculated from the retention time of the trace gas that was injected into the test column.

$$V_N = K_C \cdot V_M = \left(\frac{t_r}{t_m} - 1 \right) \cdot V_M \quad (12)$$

In the above equation, $K_C = \left(\frac{t_r}{t_m} - 1 \right)$, is the capacity factor, V_M is the volume of the mobile phase and t_r and t_m are the retention time of the probe gas and the retention time of the non-retained tracer, which was methane in this experiment.

The volume of the mobile phase is theoretically the volume available for the probe gas and the carrier gas for transport in the column.

$$V_M (cm^3 / g) = \frac{(V_{Column} - V_{packing})}{Mass\ of\ packing} \quad (13)$$

3.5 Gibbs-Helmholtz Equation

From thermodynamics, we know that $(\partial G / \partial T)_p = -S$, at constant pressure and increasing temperature, G should decrease and hence indicating greater degree of spontaneity with increasing S . Hence, we can rewrite the above equation for finite changes as follows,

$$\left(\frac{\partial \Delta G}{\partial T} \right)_p = -\Delta S \quad (14)$$

We also have another fundamental thermodynamic equation, which is

$$\Delta G = \Delta H - T\Delta S \quad (15)$$

Differentiating equation (14) and then substituting equation (15) we get equation (16),

$$\left(\frac{\partial \left(\frac{\Delta G}{T} \right)}{\partial T} \right)_p = -\frac{\Delta G}{T^2} + \frac{1}{T} \left(\frac{\partial \Delta G}{\partial T} \right) \quad (16)$$

$$\left[\frac{\partial \left(\frac{\Delta G}{T} \right)}{\partial T} \right]_p = -\frac{\Delta H}{T^2} \quad (17)$$

Substituting equation for the standard state Gibbs free energy for the transfer of molecule from the bulk air to the air-water interface, which is given as follows, $(\partial G/\partial P)_T = V$ and is written as follows,

$$\Delta G = \int_{p_1}^{p_2} V dp = RT \ln \left(\frac{p_2}{p_1} \right) \quad (18)$$

Before getting our standard state Gibbs free energy to our required final form for gas-water interface thermodynamic analysis, we should turn our attention to the chemical potentials of all the molecule of interests in all the three phases present, namely gas, water and its interface. The two bulk phase chemical potentials can be written as follows,

$$\mu_i^g = \mu_i^{0,g} + RT \ln \left(\frac{p_i}{p^0} \right) \quad (19)$$

$$\mu_i^w = \mu_i^{0,w} + RT \ln \left(\frac{a_i}{a^0} \right) \quad (20)$$

Where, $p^0 = 101.325 \text{ kPa}$ and $a^0 = 1\text{M}$, are the standard pressure and standard activity respectively. The solution activity can further be written as $a_i = \gamma_i M_i$, where the γ_i represents the concentration dependent activity coefficients and M_i represents the solute concentration in mol/L.

Similarly, we can write the chemical potentials at the interface as follows, but since the liquid near the surface is different from the liquid in the bulk, we need to account for the non-ideality of the interface with the respective surface activity coefficient, γ_i^σ . As a result we have,

$$\mu_i^\sigma = \mu_i^{0,\sigma} + RT \ln \left(\gamma_i^\sigma \frac{(\sigma_i^0 - \sigma_i)}{\pi^0} \right) \quad (21)$$

In the above equation π^0 is the standard state surface pressure for the gas phase, (=0.06084 dyne/cm), given by [Kemball and Rideal, 1946](#). While, the surface pressure analogous to bulk gas phase pressure p is $\pi = (\sigma^0 - \sigma)$, where σ^0 is the surface tension of the pure liquid and σ is the surface tension of the liquid in the adsorbed phase. Also we note that the interface is a two-dimensional form of the three-dimensional bulk phase. Hence, the Gibbs adsorption equation from the relation of the surface pressure with the surface tension, $\partial\pi = -\partial\sigma$ can be written as

$$\Gamma_i = -\frac{d\sigma}{d\mu_i} = -\frac{C_i}{RT} \frac{d\sigma}{dC_i} = \frac{C_i}{RT} \frac{d\pi}{dC_i} \quad (22)$$

From ideal gas law for the interface we have $\pi A_s = n_i^\Gamma RT$ where A_s is the surface area of the interface. Which can be written as follows,

$$\pi = \frac{n_i^\Gamma}{A_s} RT = \Gamma_i RT \quad (23)$$

Equation (22) is rewritten in the form as follows

$$\frac{d\pi}{dC_i} = \frac{RT \Gamma_i}{C_i} = \frac{\pi_i}{C} \quad (24)$$

Integrating the above equation yields the following relation and using equation (23) we have the following relation

$$\begin{aligned}\pi &= K^* C_i \\ \Gamma_i &= \frac{\pi_i}{RT} = \frac{K^*}{RT} C_i \\ \Gamma_i &= K_{LA} C_i\end{aligned}\quad (25)$$

The free energy of transfer of 1 mol of species from the gas phase to the surface is given by the following equation

$$\Delta G = \mu_i^\sigma - \mu_i^g = (\mu_i^{0,\sigma} - \mu_i^{0,g}) + RT \ln \left[\frac{\left(\frac{\gamma_i^\sigma \pi_i}{\pi_0} \right)}{\left(\frac{p_i}{p^0} \right)} \right] \quad (26)$$

At equilibrium, the first term in the above equation is zero and hence reduces to the following,

$$\Delta G^0 = (\mu_i^{0,\sigma} - \mu_i^{0,g}) = -RT \ln \left[\frac{\left(\frac{\gamma_i^\sigma \pi_i}{\pi_0} \right)}{\left(\frac{p_i}{p^0} \right)} \right] \quad (27)$$

The surface activity coefficients γ_i^σ is a function of the surface coverage or surface pressure π_i , and tends to 1 as π_i tends to zero. Hence the above equation reduces to the following form

$$\Delta G^0 = -RT \ln \left[\frac{\left(\frac{\pi_i}{\pi_0} \right)}{\left(\frac{p_i}{p^0} \right)} \right] = -RT \ln \left[\left(\frac{\pi_i}{p_i} \right) \left(\frac{p_0}{\pi_0} \right) \right] \quad (28)$$

The ratio (p_0/π_0) is the ratio of the standard states called the standard surface thickness, where, p_0 is the standard state pressure equal to 101.325 kPa, and π_0 (=0.06084 mN/m), is the standard state surface pressure given by ([Kemball and Rideal, 1946](#)). Hence the ratio, ($p_0/\pi_0 = \delta_0$), is equal to 6×10^{-10} m. Also the ratio π_i/p_i for an ideal gaseous state can be written as π_i/C_i , which is equal to the partition constant K_{IA} defined in equation (11) with units of length. Hence the equation simplifies to the form in which we want as follows

$$\Delta G_{IA}^0 = -RT \ln \left[K_{IA} \left(\frac{p_0}{\pi_0} \right) \right] = -RT \ln \left[\frac{K_{IA}}{\delta_0} \right] \quad (29)$$

Using the integral form of the Gibbs-Helmholtz equation in equation (17), and the relation for the standard state Gibbs free energy in equation (29) we can obtain the following equation

$$\left[\frac{\partial \left(\ln \frac{K_{IA}}{\delta_0} \right)}{\partial T} \right]_p = \frac{\Delta H_{IA}}{RT^2} \quad (30)$$

Which upon integration yields the following equation used to obtain the required thermodynamic parameters from the results of the IGC technique.

$$\ln \left(\frac{K_{IA}(T)}{\delta_0} \right) = -\frac{\Delta H_{IA}}{RT} + Const. \quad (31)$$

In the above equation, the partition constant K_{IA} at the gas-water interface is obtained from the equation (10). A plot of $\ln(K_{IA}/\delta_0)$ as a function of $(1/T)$ will yield the heat of adsorption ΔH_{IA} .

3.6 Gas-Solid Interface

In order to show the significance of a gas-water interface, it is essential to determine the thermodynamic functions for a gas-solid interface. In addition, there are no previous data on the adsorption of compounds considered in this work on a gas-water interface. Hence, the IGC methodology can be validated with data on gas-solid adsorption from other work.

A solid by definition is a matter that is rigid and resists stress. The adsorption of matter on a solid and a gas-solid interface has been a subject of interest, and can be dated back to the classical work of [Langmuir, 1918](#) and [Brunauer, Emmett and Teller, 1938](#). Typically, both physical adsorption and chemical adsorption are processes observed at a gas-solid interface.

3.7 Theory of Adsorption

Adsorption of a gas is always an outcome of attractive forces between individual molecules of the gas and the atoms or ions composing the solid. The forces that bring about adsorption always include dispersion forces together with short-range repulsive forces. Rapid fluctuation in electron density within each atom induces an electrical moment leading to attraction between two atoms, resulting in “non-specific” adsorption. Columbic forces result in “specific” adsorption. In a polar solid, containing ions, with polar groups or π -electrons, it will result in an electric field that will induce a dipole in the adsorbent.

Adsorbents are divided into three classes namely,

- (1) No ions or positive groups (graphitized carbon)
- (2) Concentrated positive charges (OH groups on hydroxylated oxides)

(3) Concentrated negative charges (=O, =CO).

Adsorbates are divided into four groups:

- (1) Spherically symmetrical shells or F-bonds (noble gases, saturated hydrocarbon)
- (b) B-bonds (unsaturated or aromatic hydrocarbons) or lone pair of electrons (ethers and tertiary amines)
- (c) Positive charges concentrated on peripheries of molecules
- (d) Functional groups with both electron density and positive charges concentrated as above (molecules with -OH or =NH groups).

3.8 Adsorption on Dry Diatomaceous Earth

The adsorption on solid surfaces is dependent on the surface morphology and the chemical composition of the solid. The diatomaceous earth considered in this work is primarily made of silanol groups. The interaction of silanol groups with aromatic hydrocarbons is established by hydrogen bonds to aromatic π -system, resulting in flat adsorption configuration ([Pohle, 1982](#)). Benzene interacts with silica surface predominantly through dispersion forces and this interaction is strongest when the benzene molecule is able to lie with its plane flat against the silica surface ([Bilinski et al, 1998](#)). The jump probability (mobility) of benzene is enhanced in a irregular surface in comparison to a flat surface.

CHAPTER 4

EXPERIMENTAL METHODOLOGY

4.1 Sample Probe Gas Preparation

4.1.1 Benzene Vapor Probe Preparation

The pure sample of Benzene used in this work was obtained from Fisher Scientific Company at 99% purity. Since benzene has relatively higher vapor pressure than the other two PAHs, sample probes of benzene were obtained in the vapor phase from a closed bottle containing the pure compound that was maintained in a temperature controlled bath at about 50 °C. A gastight syringe was used to obtain the required amount of the vapor sample from the bottle and was then inject it into the gas chromatograph column. This method worked well for benzene due to its high vapor pressure and Henry's constant. The Henry's constant for various volatile and semi-volatile organic compounds are determined in this manner ([Cheng et al, 2003](#)).

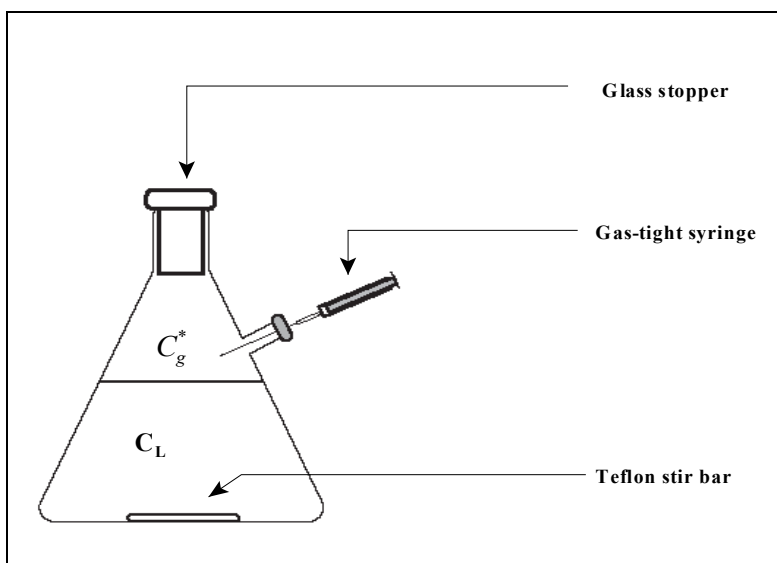


Figure 7 Preparation of organic vapors from flasks maintained in temperature controlled ovens.

4.1.2 Naphthalene and Phenanthrene Vapor Probe Preparation

The pure sample of Naphthalene was also obtained from Fisher Scientific Company at 99% purity, and phenanthrene was obtained from Aldrich chemical company at 98% purity. Initially, the same methodology used for benzene vapor sample was used for these two PAHs. Owing to the difficulty in obtaining significant (to be detected by the detector) concentration in the gas-tight syringe for the two low vapor pressure PAHs, a Pure-compound Vapor Generator (PVG) was designed. However, during the development stage of the PVG, most experimental runs were performed by placing the bottle containing the pure compound in an oven maintained at temperatures equivalent to the boiling points of the compounds. In this manner, detectable masses of vapor samples were obtained. It is important to note that though constant concentration of vapor samples were required, it was not essential to determine the concentration of the samples injected. The vapor sample preparation and the IGC experiment (column) were maintained at same temperature.

The vapor generator was made of two tubular stainless steel columns (SS 316, 0.762m long, 0.013m O.D.) connected serially and each packed with Chromosorb P (60/80 mesh non-acid washed, a porous diatomaceous support material from Supelco Inc., Bellefonte PA) coated with pure PAH compound and, with an inline static mixer in a temperature controlled environment. Chromosorb P, the packing in the chamber was coated with pure PAHs, by mixing the dry support material with a solution made by dissolving excess PAH in 100mL hexane (HPLC grade) and then dried in a fume hood until a free flowing powder was achieved.

Sample sizes injected into the GC ranged from 1×10^{-7} to 2×10^{-7} m³ for benzene and 5×10^{-7} m³ and higher for naphthalene and phenanthrene because of their low vapor pressures.

4.2 Schematics of the IGC Experiment

The vapor stream entered a Hewlett-Packard gas chromatograph (HP 5890A) that contained a stainless steel column (0.91m x 0.00635m i.d.) packed with Chromosorb P. The dry packing has a surface area of 4 to 5 m²/g, a bulk density of 0.38 g/cm³ and a mean particle density of 2.3 g/cm³. The carrier gas (helium) flow rate was about 5×10^{-5} m³/min with column head pressure maintained at 152 kPa, and the outlet pressure was atmospheric. Since water has considerable vapor pressure of 23.76 mm Hg at room temperature, the passage of dry helium would remove the water coated on the packing for test purposes. To prevent this removal of water, as shown in Figure 8, the carrier was pre-saturated with water at more or less the same temperature as the column was operated. It is also of interest to note that the sample was prepared at the same temperature as the column.

In the case of naphthalene and phenanthrene, samples were injected using a manually actuated six-port valve. The valve was connected with a 1 mL sample loop that maintain constant volume of sample injection between each experimental trial. The outlet of the injection port was connected to a vent trap made of XAD material obtained from Supelco Inc., that adsorbs PAH vapors. Since the carrier gas was saturated with water, there were some perturbations in the GC signal. Keeping the inlet temperature slightly higher than the column temperature minimized these signal perturbations.

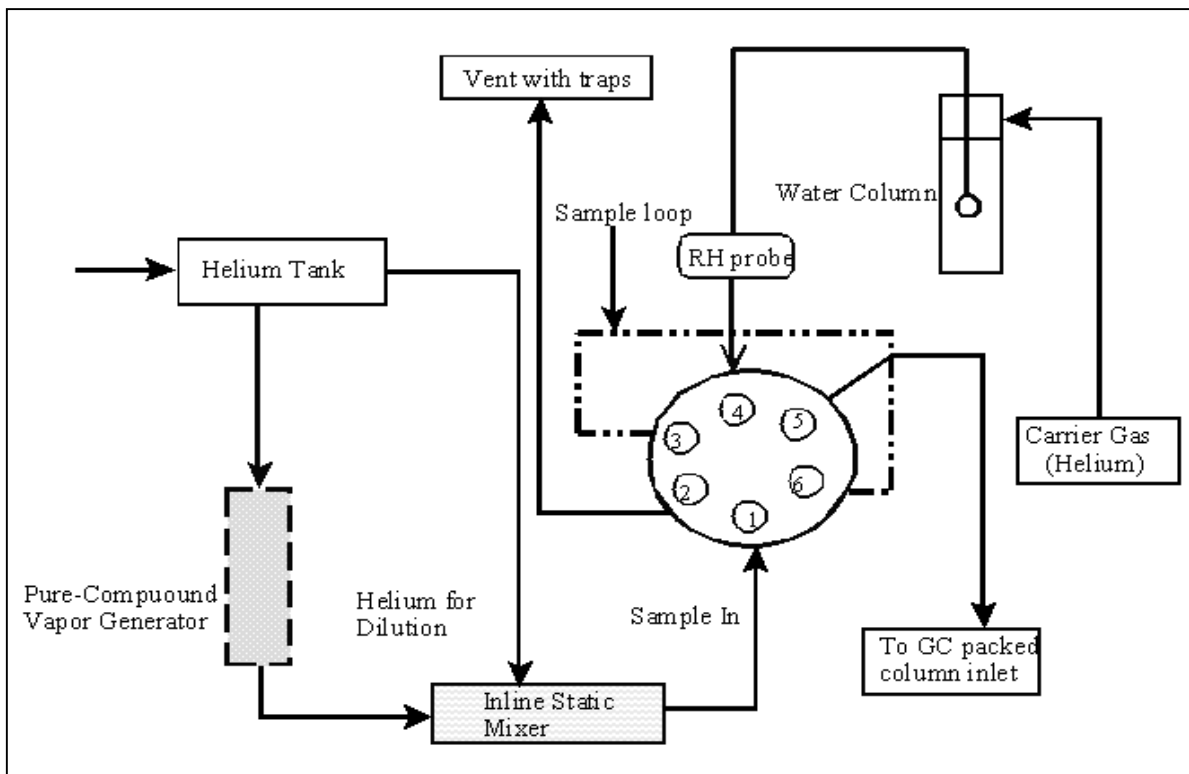


Figure 8. Schematics of the gas-water interface adsorption experiment.

4.3 Detection System

Dozens of detector have been used and investigated during the development of gas chromatography by several researchers. An ideal detector for chromatography is usually characterized with adequate sensitivity, good stability, linear response over a good range of solute masses, short response time and high reliability. Needless to say no detector exhibits all these characteristics.

Nonetheless, the Flame Ionization Detector (FID) has found wide use and is generally applicable for most gas-chromatographic applications. A typical Hewlett Packard company FID detector is shown in Figure 9. The effluent from the column is mixed with hydrogen and air and then ignited electrically. Most organic compounds when pyrolyzed at the temperature of a hydrogen/air flame produce ions and electrons

that can conduct electricity through flame. A potential of few hundred volts is applied across the burner tip and a collector electrode located above the flame. The resulting generated current, about 10^{-12} Amps, between the two electrodes is directly proportional to the hydrocarbon concentration in the sample that is burned by the flame. A high-impedance operational amplifier measures the signal. Because the FID responds to the number of carbon atoms entering the detector per unit time, it is a mass sensitive, rather than a concentration sensitive, detector.

The flame ionization detector has high sensitivity of $\sim 10^{-13}$ g/s, a large linear response and low noise ([Skoog et al, 1998](#)). FID is rugged and easy to use, but it is destructive of sample. Other detectors that were available were thermal conductivity detector, sulfur chemi-luminescence detector, electron capture detector and atomic emission detector. Of the numerous detectors available, FID is the most suitable for organic compounds.

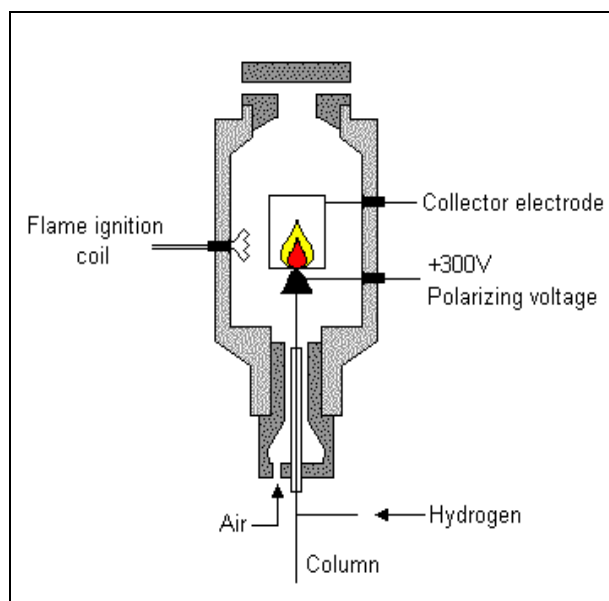


Figure 9. Flame ionization detector

The sample compounds that were injected in to the packed column were thus detected at the outlet of the column using this Flame Ionization Detector (FID). The retention time of each of the samples injected was recorded using Hewlett Packard Computer program that interfaced the desktop computer and the GC.

4.4 Gas Chromatographic Columns

Gas chromatographic applications generally employ two types of columns, packed columns and open tubular capillary columns. Since we are employing Inverse gas chromatography (IGC), in which the stationary phase is to be studied (adsorption of organic vapors to gas-water interface) by the passage of volatile probe molecules (organic vapors) carried through the column by the inert carrier gas. A stainless steel tubular column was packed with water-coated Chromosorb P, a porous diatomaceous earth obtained from Supelco Inc.

4.4.1 Water Coated Column Preparation

The packing material was washed thoroughly in the HPLC grade water and dried in an oven overnight and cooled in a desiccator. The clean dry material was loaded with a measured quantity of distilled de-ionized HPLC grade water. The mass of water loaded was checked by weighing the sample of the material before and after drying the samples at 100 °C for about 6 hours. The water loaded packing material was filled into the stainless column by gentle suction. Inevitably, water was lost from the packing and in order to ascertain the actual water loading the samples were weighed before and then after column were filled. As a result, the water loading obtained ranged from 0.036 to 0.38 mass of water per unit mass of support.

CHAPTER 5

RESULTS AND DISCUSSION

5.1 Adsorption of Organic Compounds on Gas-Solid Interface

A series of experiments were performed on dry column to study the adsorption of organic compounds to gas-solid interface. In this case the equation (10) in Chapter 2 can be applied by neglecting the partitioning into the bulk water and using the surface area A_S of the dry packing instead of A_W . The modified equation for the study of gas-solid adsorption is written as follows

$$V_N (cm^3 / g) = K_{SA} A_S \quad (32)$$

In the above equation K_{SA} is the gas-solid partition constant for the solute and the surface area for the dry packing as reported by the manufacturing company to be 50×10^3 cm^2/g was used. The adsorption from gas phase to solid or liquid is commonly described by an the adsorption or the gas-solid partition constant,

$$K_{SA} (\mu m) = \frac{\text{amount of adsorbate } i \text{ per surface area of adsorbent (mol / m}^2\text{)}}{\text{amount of adsorbate } i \text{ per volume of gas (mol / m}^3\text{)}}$$

The dependence of temperature on K_{SA} is given by the analogous Van't Hoff equation, ([Goss, 1994](#), [Goss and Schwarzenbach, 1999](#)) have shown a correlation for heat of adsorption as function of K_{SA} using the Van't Hoff equation below,

$$\ln \left(\frac{K_{SA}(T_2)}{K_{SA}(T_1)} \right) = \frac{\Delta H_{SA}}{R} \left(\frac{1}{T_1} - \frac{1}{T_2} \right) \quad (33)$$

5.2 Adsorption of Benzene at Gas-Solid Interface

25 μ L samples of benzene vapor, obtained from the vapor phase using a gas-tight syringe, were injected into the packed column. The column used in the study of gas-solid interface was packed with dry Chromosorb and installed in the gas chromatograph. The retention times of the benzene samples injected were recorded at various temperatures and the capacity factor K_C was computed using the retention times of the probe and un-retained tracer as $K_C = \left(\frac{t_r}{t_m} - 1 \right)$. The samples for benzene were prepared from as low as room temperature to a high 100 $^{\circ}$ C. The column temperature as well as the sample preparation temperatures were maintained the same each set of experiments. A plot of the $\text{Log}(K_C)$ versus $1/T$ is shown in the Figure 10. The slope of the equation indicated in the plot is used to compute the heat of adsorption on the gas-solid interface.

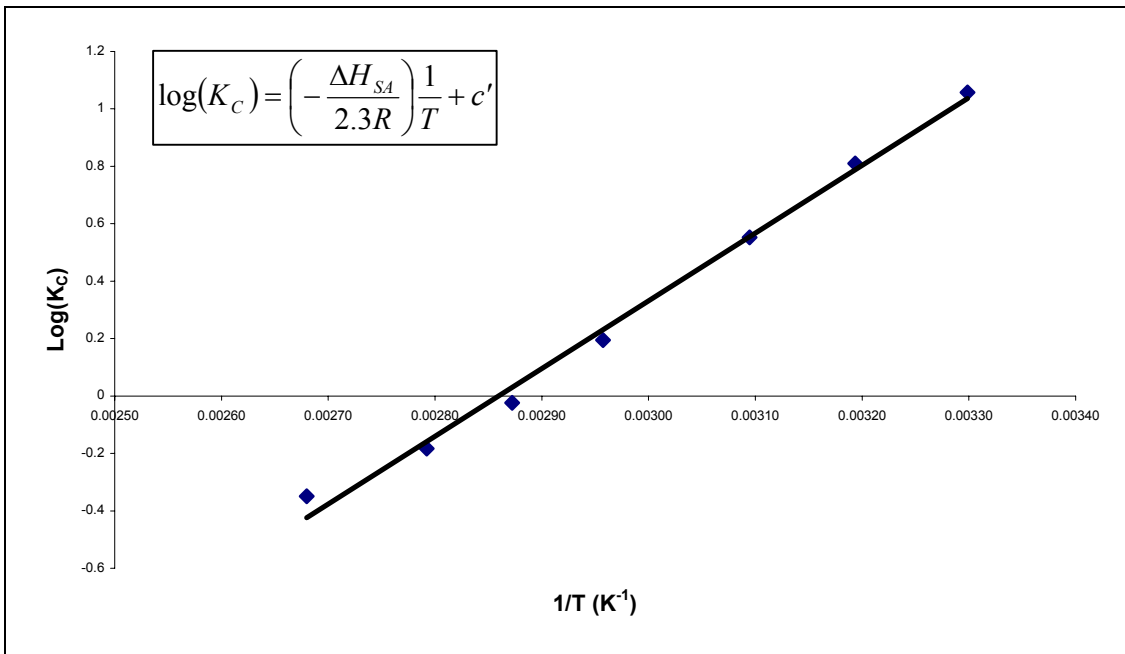


Figure 10. Heat of adsorption of benzene on a gas-solid interface ($R^2=0.9932$).

In the case of a dry solid interface the equation (30) in Chapter 3 is written down in a form that does not consider the partitioning to the bulk water phase. Hence the temperature dependence of the equilibrium constant is given by the Van't Hoff equation, assuming that the adsorption is constant over the temperature range considered, as in equation (34). The slope is used to determine the heat of adsorption while the intercept can be simplified to yield $-\Delta S^0/R$.

$$\log(K_c) = \left(-\frac{\Delta H_{SA}}{2.3R} \right) \frac{1}{T} + c' \quad (34)$$

After having obtained an average value for the heat of adsorption by this method of linear regression, equation (8) in Chapter 2 was used to obtain the standard free entropy of adsorption. The heat of adsorption on a dry solid obtained this way was -45 ± 2 (kJ/mol). The free energy was calculated from the equation, $\Delta G_{SA}^0 = -RT \ln \left[\frac{K_{SA}}{\delta_0} \right]$, where $\delta_0 = 6 \times 10^8$ ([Kemball and Rideal, 1946](#)) derived in Chapter 3. The standard entropy was calculated from the equation, $\Delta S_{SA} = \frac{1}{T} (\Delta H_{SA} - \Delta G_{SA})$. The standard free entropy of adsorption obtained was -73 ± 1 (J/K·mol). The computed data is listed in Table 7 along with data of other compounds.

5.3 Adsorption of Naphthalene at Gas-Solid Interface

In the case of naphthalene, which is known to be more hydrophobic, and of lower vapor pressure, obtaining reproducible concentration from a bottle containing the pure component was seldom possible without having the compound in a water bath. Nevertheless, when the samples were prepared at the same temperatures as column

temperatures were operated, it seemingly reduced the deviations in results from each experiment.

The initial operating system temperature, which here refers to the sample preparation temperature and the GC column operating temperature, were elevated to almost two orders of magnitude higher in comparison to the working temperature for the benzene and also were successively increased to obtain a linear plot shown in Figure 11. The slope of the regression equation gives the heat of adsorption as shown in plot, where K_C is the capacity factor calculated the retention time of the naphthalene and the unretained peak, methane. The heat of adsorption obtained from the above plot was -80 ± 2 (kJ/mol) and the standard entropy of adsorption was -95 ± 5 (J/K·mol).

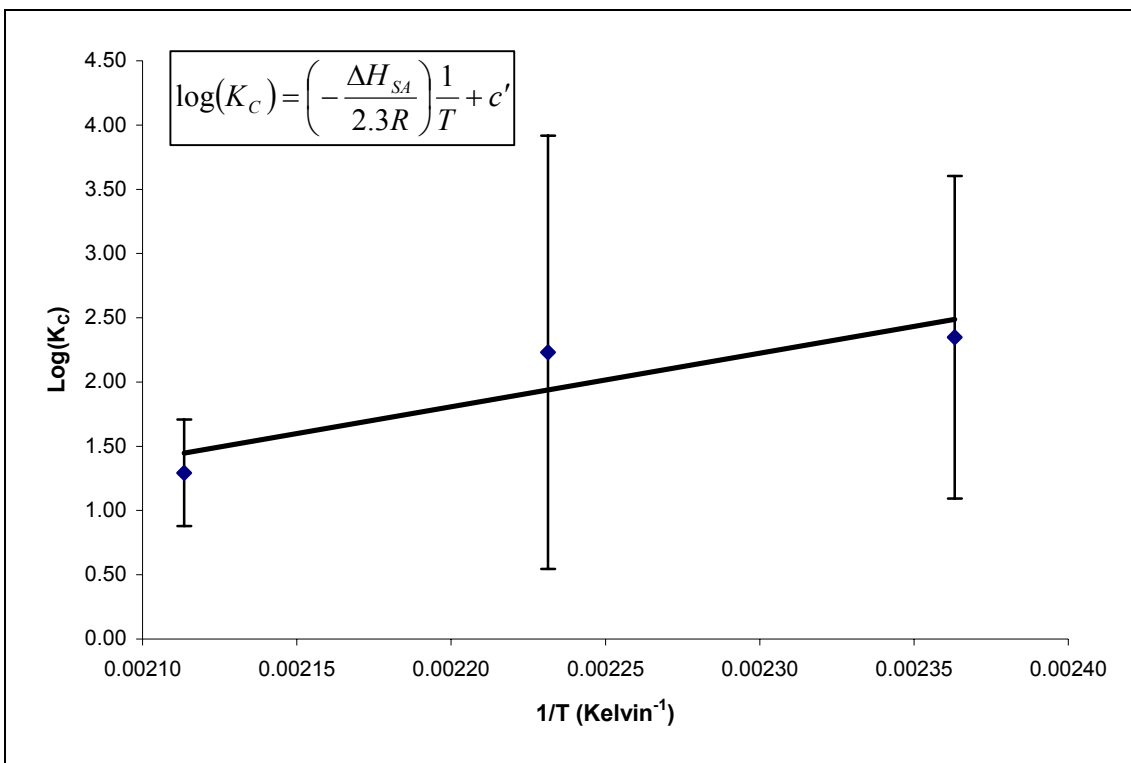


Figure 11. Heat of adsorption of naphthalene on a gas-solid interface ($R^2=0.8075$).

5.4 Adsorption of Phenanthrene at Gas-Solid Interface

In the case of phenanthrene the operating temperatures were 175 °C to 225 °C and the repeatability of the gas concentration were relatively good and this can be seen from the linearity of the Van't Hoff's plot with a correlation of $R^2=0.99$. The heat of adsorption of phenanthrene on the gas-solid interface was calculated to be -116.1 ± 0.3 (kJ/mol) while the entropy of adsorption was -152 ± 5 (J/K·mol). A table of data for phenanthrene is attached for various temperatures studied.

In Table 2, T is the system temperature that includes the sample preparation temperature and the column temperature, T_R is the retention time of the probe gas, K_C is the capacity factor that include the retention time of the tracer and un-retained gas (methane) and was discussed in the previous section. Using the above data, a linear plot of Gibbs Helmholtz equation can be obtained as shown in Figures 12.

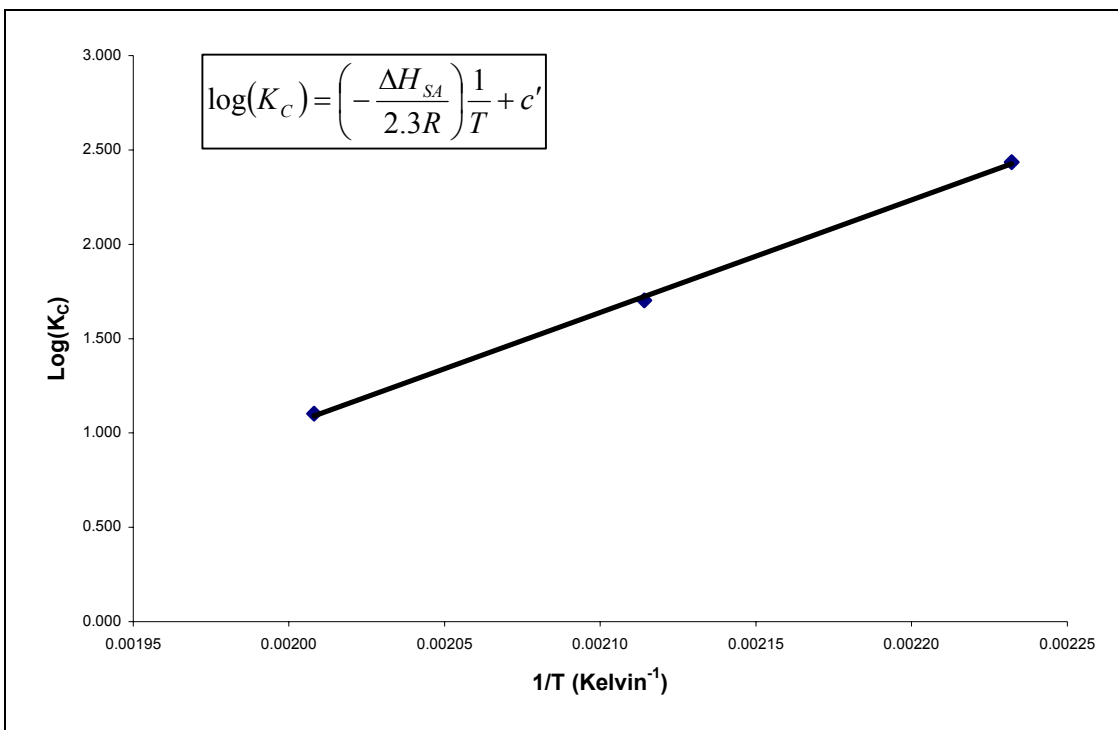


Figure 12. Heat of adsorption of phenanthrene on a gas-solid interface ($R^2=0.9993$).

TABLE 2. PHENANTHRENE GAS-SOLID ADSORPTION EXPERIMENTS

T (Kelvin)	1/T (Kelvin) ⁻¹	T _R (min)	K _C	Log (K _C)
175	0.00223	172	272.885	2.436
200	0.00211	30	50.370	1.702
225	0.00201	7.7	12.652	1.102

5.5 Analysis of Gas-Solid Adsorption Results

From the experiments performed on a dry column, the enthalpy and entropy of adsorption was calculated and is summarized in Table 3. It can be observed that the change in enthalpy of adsorption is about 35 kJ/mol per aromatic ring. Adsorptions of aromatic hydrocarbons were done on dry soil, and [De Seze, 1999](#) obtained an increase of 41kJ/mol enthalpy of adsorption per aromatic ring. The heat of adsorption is related to the strength with which the adsorbate molecules are bonded to the active surface. It is apparent from the data that as the molecule becomes larger, the enthalpy of adsorption and the entropy become more negative indicating that the molecules are favorably adsorbed.

The difference in chemical potential, $\Delta\mu$, between the gas at the standard pressure p_0 and at equilibrium is

$$\Delta\mu = \mu_s - \mu_g^0 = RT \ln\left(\frac{p}{p_0}\right) \quad (35)$$

and $\Delta\mu$ (i.e. ΔG) measures the affinity between adsorbate and adsorbent at the coverage corresponding with the equilibrium pressure p ([Barrer, 1966](#)). In the above equation, μ_s is the chemical potential of the adsorbed gas and μ_g^0 is the chemical potential of the gas in the gas phase at pressure p_0 . From the above equation we can rewrite as follows,

$$\Delta\mu = \Delta H_{SA} - T\Delta S_{SA} \quad (36)$$

The difference in chemical potential indicate more negative value as the hydrophobicity of the compound increases, indicating that de-sorption is more difficult for Benzene than for phenanthrene. The higher value of K_{SA} , together with a more negative value for the $\Delta\mu$ ($=\Delta G$) for phenanthrene, indicates that the adsorption is more favorable for the most hydrophobic compound. Also, a more negative value for $\Delta\mu$ in the case of phenanthrene distinctly indicates that not only there is lesser affinity for the adsorbate and adsorbent, but also there is greater mobility of adsorbed phenanthrene on the various adsorption sites than for benzene. Thus, from the adsorption enthalpy being more negative for phenanthrene indicates the binding strength of this compound to be larger than for benzene. A preliminary confirmation of this GC methodology has been validated by the similar trend in results from the experiments of [De Seze, 1999](#).

TABLE 3. GAS-SOLID ADSORPTION THERMODYNAMICS OF AROMATIC HYDROCARBONS.

Property	Benzene	Naphthalene	Phenanthrene
K_{SA} (μm) at 298 K	5.36	105.02	1.88×10^9
Enthalpy of adsorption (ΔH_{SA}) [kJ/mol]	-45 ± 2	-80 ± 2	-116.1 ± 0.3
Entropy of adsorption (ΔS_{SA}) [J/K·mol]	-73 ± 1	-95 ± 5	-152 ± 5
Difference in Chemical potential ($\Delta\mu_{SA}$) [kJ/mol]	-23 ± 2	-51 ± 2	-70 ± 1

5.6 Adsorption of Organic Compounds at Gas-Water Interface

In Chapter 2, a detailed development of the thermodynamic analysis was presented on the gas-water interface dynamics. The column installed in the gas chromatograph was packed with known quantities of water as mentioned in the experimental section.

5.6.1 Determination of Specific Surface Area of Water Loaded Column Packing

In order to obtain the specific surface areas of the water coated packing the retention volume of a fixed volume and concentration of heptane was injected into the column filled with water-coated packing, assuming that the partitioning of heptanes to bulk water is negligible, and is demonstrated by the literature value of K_{WA} ([Hartkopf and Karger, 1973](#) and [Hoff et al, 1993](#)). Hence, equation 10 in Chapter 2, simplifies as follows,

$$\begin{aligned}\frac{V_N}{V_w} &= K_{IA} \frac{A_w}{V_w} \\ A_w &= \frac{V_N}{K_{IA}}\end{aligned}\tag{37}$$

In the above equation V_N is the retention volume computed from the retention time of Heptane in the column, and K_{IA} is the known interface partition constant obtained from [Hoff et al, 1993](#). Heptane was injected for different water loadings and Figure 13 is a linear regression plot of the data obtained.

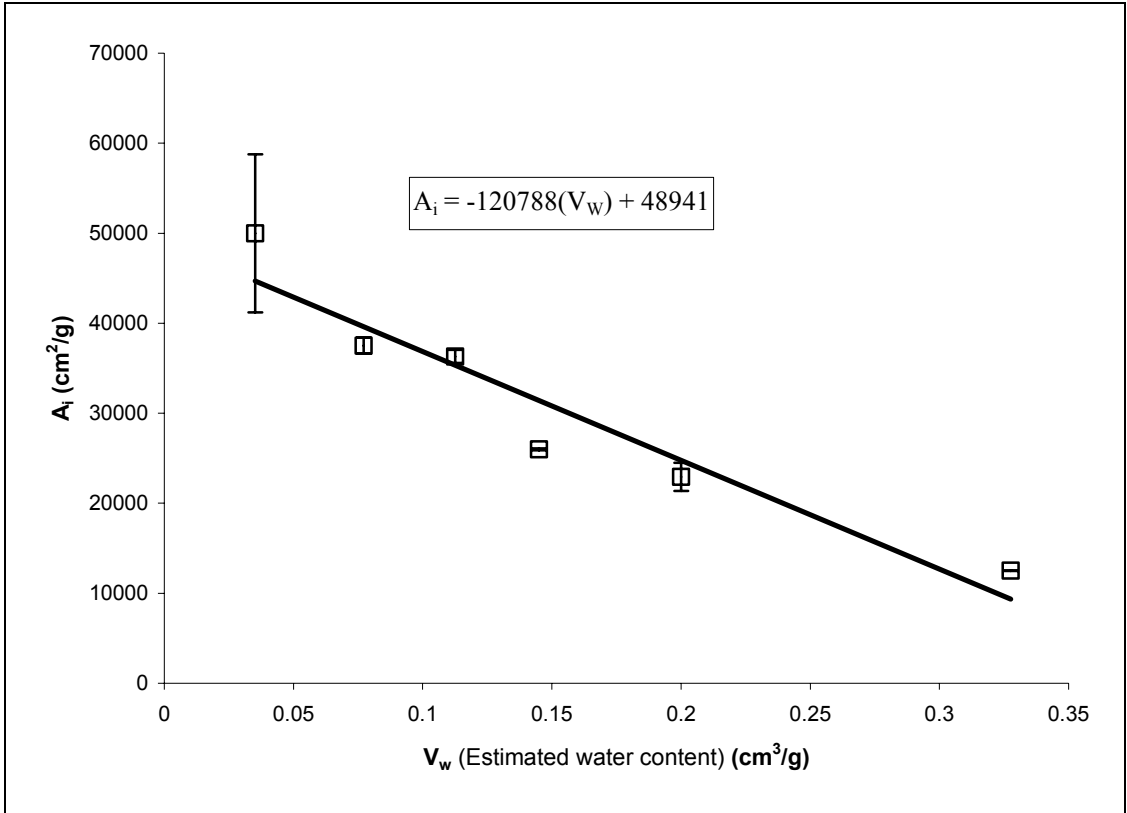


Figure 13. Estimation of specific surface area of water loaded packing ($R^2=0.912$).

In Figure 13, the dry packing ($V_w=0$) extrapolates to the manufacturing company reported surface area data of $50 \times 10^3 \text{ cm}^2/\text{g}$. The correlation equation indicated in the plot was directly used to obtain the specific surface area of the water-loaded packing, when the water loaded on the packing was estimated. The mass of water loaded was estimated by weighing samples of the water-coated material and drying them at $100 \text{ }^\circ\text{C}$ for about 6 h.

5.7 Adsorption of Benzene in Gas-Water interface

Adsorption of the organic vapor occurs on the gas-water interface of the support with simultaneous dissolution in the bulk water present on the surface. Equation (10) is

$$\text{rewritten as, } \frac{V_N}{V_W} = K_{IA} \frac{A_W}{V_W} + K_{WA}.$$

In order to obtain the K_{IA} from the above equation, packed columns were prepared with various water loadings and the water loadings V_W , which is the weight of water per gram of dry packing, were estimated experimentally. The specific surface area for the various water-loaded packing was estimated using the correlation in Figure 11.

Samples of benzene were injected into each column successively and the retention times were recorded to calculate the retention volume V_N . Figure 12 shows the plot of equation (37) for benzene at 298 K and its applicability to extract the partition constant for the partitioning at the gas-water interface. The value of K_{IA} obtained from this linear regression was $0.43 \pm 0.01 \mu\text{m}$ and the value of K_{WA} obtained for benzene was 5.2. The experiment was repeated for different temperatures to obtain the temperature variation in K_{IA} . The plot of the experimental results for K_{IA} at various water loadings is shown in Figure 13. Table 4 shows the experimental results for K_{IA} at various temperatures.

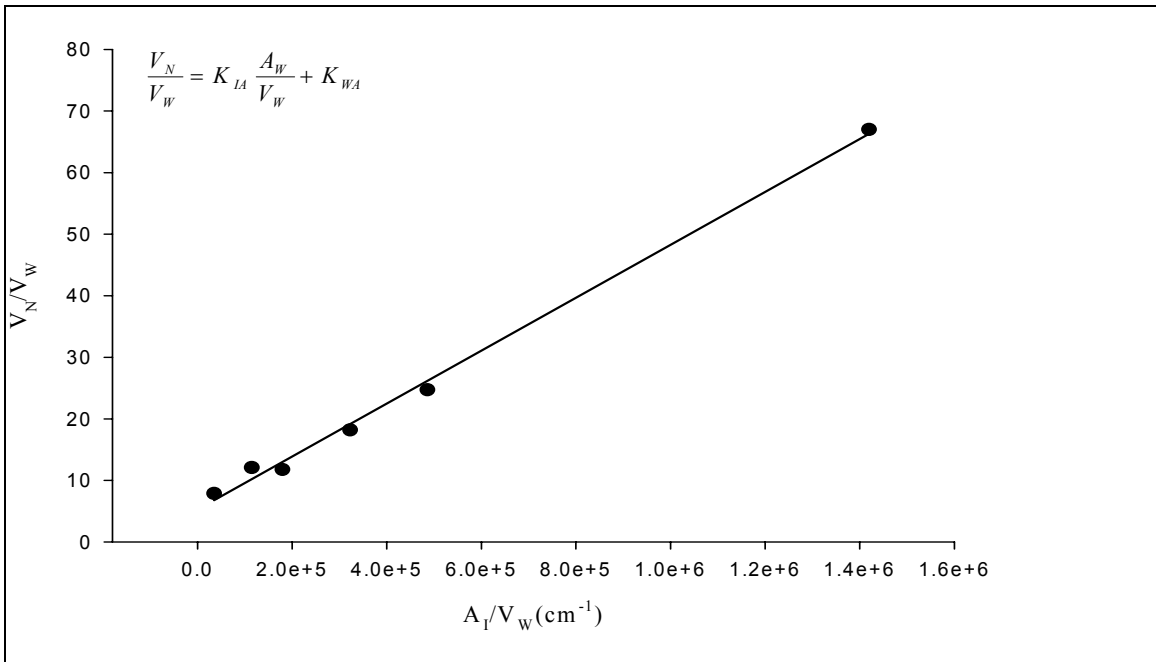


Figure 14. Plot of V_N/V_W versus A_W/V_W for benzene at 298 K ($R^2 = 0.996$)

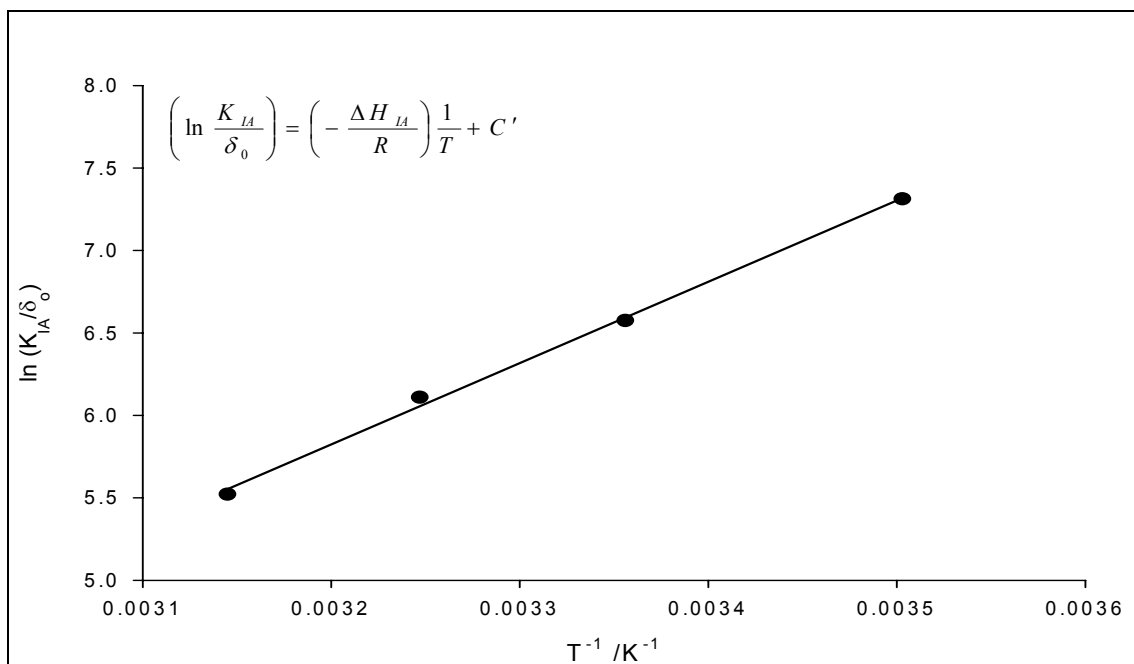


Figure 15. Integral form of the Gibbs-Helmholtz equation for benzene ($R^2=0.998$).

TABLE 4. BENZENE PARTITION CONSTANT AS FUNCTION OF TEMPERATURE.

Temperature (Kelvin)	K_{IA} (μm)	ΔG_{IA} (kJ/mol)
298	0.43	-16.3
308	0.20	-14.9
318	0.09	-13.2

Figure 14 shows a plot of the Gibbs-Helmholtz equation to obtain the heat of adsorption. The free energy and entropy of adsorption were calculated using equation shown previously. The variation of K_{IA} show a decreasing trend with temperature, and this can attributed to the decrease in surface adsorption. The free energy at 298K is more negative than at higher temperatures, indicating adsorption is favored at the lower temperature. The free energy being more negative at lower temperatures indicates higher surface mobility at higher temperature, known as adsorbate induced restructuring of

surface ([Adamson, 1982](#)). A direct consequence of this surface mobility, in our context of gas-water interface of environmental systems, only owes to the negative trend of surface adsorption with temperature, and hence on the scavenging efficiency in wet deposition.

The free energy value obtained for benzene, -16.3 kJ/mol, is in good agreement with other reported values in the literature. Using axisymmetric drop shape analysis, [Braunt and Conklin, 2000](#) obtained -16.3 kJ/mol, which is in excellent agreement with this work. Using molecular dynamics simulations [Dang and Feller, 2000](#) reported a value of -16.6 kJ/mol. Their molecular dynamics simulations reveal that the benzene molecule was parallel to the interface when the molecule was located at the minimum of the free energy profile with an adsorption free energy similar to the value obtained in this work.

Another important aspect of the gas-water adsorption at the interface in the IGC technique is to ascertain the linearity of the adsorption isotherm ([Brunauer, Emmett and Teller, 1938](#)). The vapor concentration of the compound injected onto the inlet of the GC column was varied and the chromatograms for the various vapor concentrations are shown in Figure 14. No significant variations in peak shape or retention time is observed in the chromatograms below confirming the linearity of the adsorption isotherm.

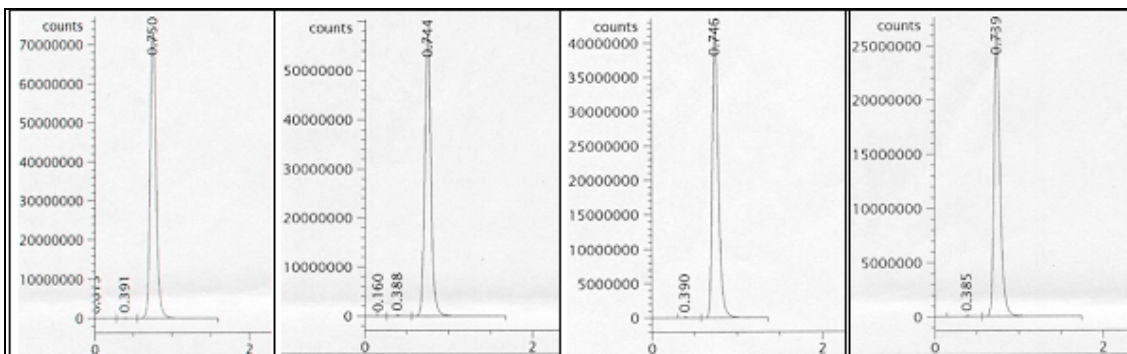


Figure 16. Benzene vapor injection volumes 25 µl to 100 µl (Water loading= 0.32 g/g, 298 K)

5.8 Adsorption of Naphthalene at the Gas-Water Interface

Samples of naphthalene vapor were injected into the packed column for various water loadings on the packing materials. Plot of V_N/V_W versus A_W/V_W for naphthalene is shown in Figure 17. The linear regression of equation (37) yielded the partition constant K_{IA} for naphthalene at 298 Kelvin to be $27.2 \pm 1.8 \mu\text{m}$. Table 5 shows the K_{IA} for various temperatures determined in this work.

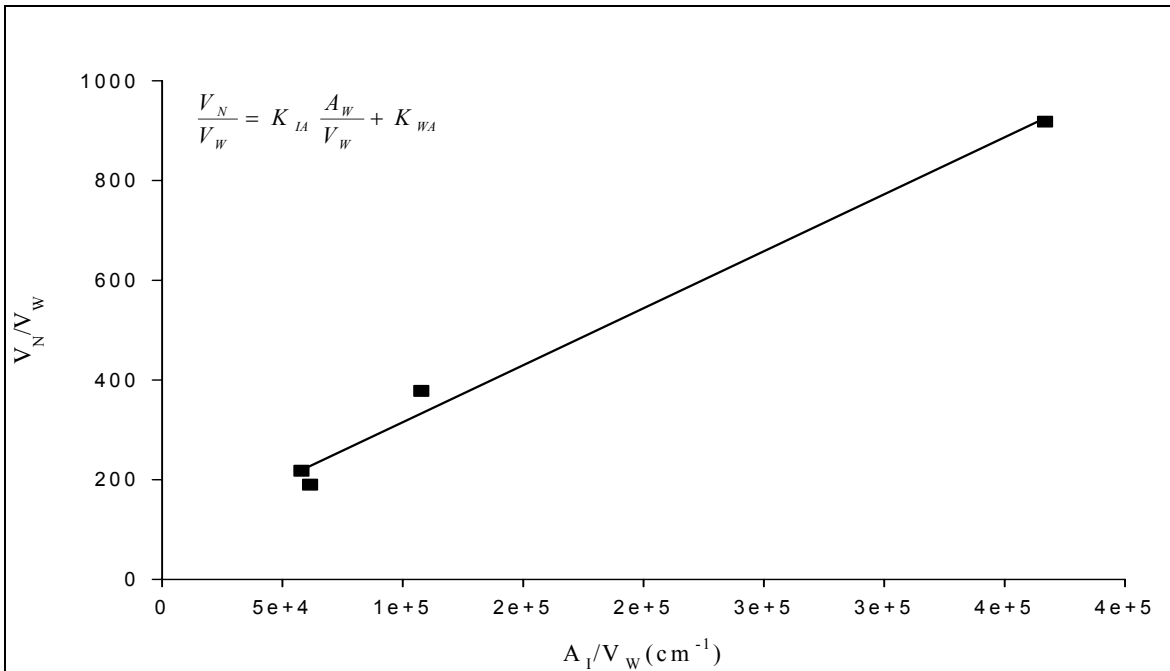


Figure 17. Plot of V_N/V_W versus A_W/V_W for naphthalene at 298 K ($R^2 = 0.992$).

The partition constant K_{IA} , obtained at various temperatures are plotted in Figure 18, which is an illustration of the Gibbs-Helmholtz equation for naphthalene. The slope of the equation will yield the heat of adsorption at the gas-water interface. The Entropy of adsorption is calculated from equation, $\Delta S_{IA} = \frac{1}{T}(\Delta H_{IA} - \Delta G_{IA})$ and the free energy of

adsorption from equation, $\Delta G_{IA}^0 = -RT \ln \left[\frac{K_{IA}}{\delta_0} \right]$.

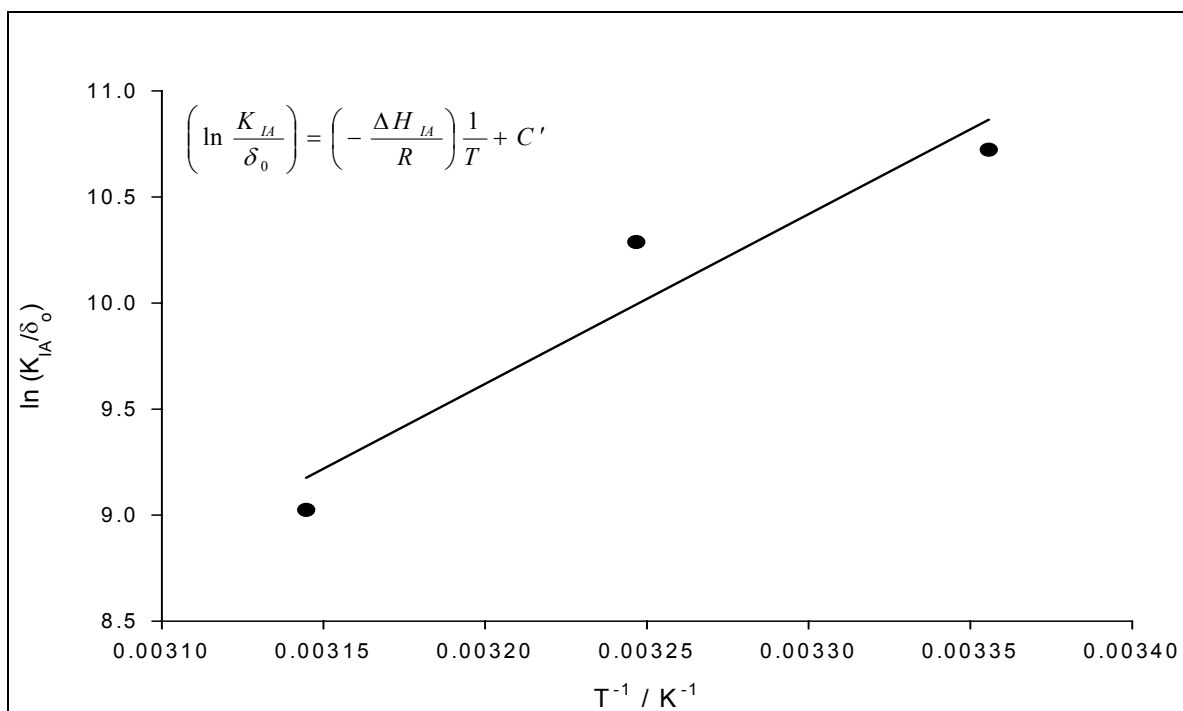


Figure 18. Integral form of the Gibbs-Helmholtz equation for naphthalene (R²=0.936).

TABLE 5. NAPHTHALENE PARTITION CONSTANT AS FUNCTION OF TEMPERATURE.

Temperature (Kelvin)	K _{IA} (μm)	ΔG _{IA} (kJ/mol)
298	27.42	-26.6
308	15.05	-25.9
318	1.22	-20.1

Table 5 lists the K_{IA} values determined for naphthalene, the partition constant for naphthalene is larger than benzene, which is a direct indication that the accumulation of this PAH is considerably larger than benzene. The interface constant K_{IA} can also be viewed as a parameter that indicates the hydrophobicity of the compound, larger the value of K_{IA} the more hydrophobic is the compound.

The free energy for naphthalene being more negative indicates that the surface restriction to the movement of adsorbed naphthalene is lesser than for benzene, and that desorption is more difficult for benzene than for naphthalene. Also, the adsorption is more favorable at lower temperature. In terms of surface mobility, smaller molecules gain entropy on desorption from the surface and dissolution into the bulk water. Since the increase in entropy is from the interface to the bulk water, as a result, the interface surface restricts the movement of the molecule much more than the bulk system. Hence, the surface mobility is more pronounced for smaller molecules than for larger molecules, and [Davies and Rideal, 1963](#) observed similar trends for smaller and larger hydrocarbon chain molecule. The value of K_{IA} at 298 K obtained for naphthalene is nearly 63 times larger than that benzene. If also naphthalene adsorbs parallel to the interface, then adsorption free energy can be expected to be proportional to molecular surface area. The molecular surface area of benzene molecule is 110 \AA^2 and that of naphthalene is 156 \AA^2 , thus the adsorption free energy can be expected to be 1.4 times larger than that of naphthalene. The experimental ratio of free energy of benzene and naphthalene is 1.6.

5.9 Adsorption of Phenanthrene at the Gas-Water Interface

In the series of organic compounds that were analyzed in this work, phenanthrene is the most hydrophobic and the lowest vapor pressure. Owing to this fact, the work with phenanthrene was far more cumbersome than with the other two hydrophobic compounds. Injection of compounds into the test columns was done using the pure compound generator as mentioned earlier in the experimental procedure method. A plot of the regression analysis for equation (37) is shown in Figure 19.

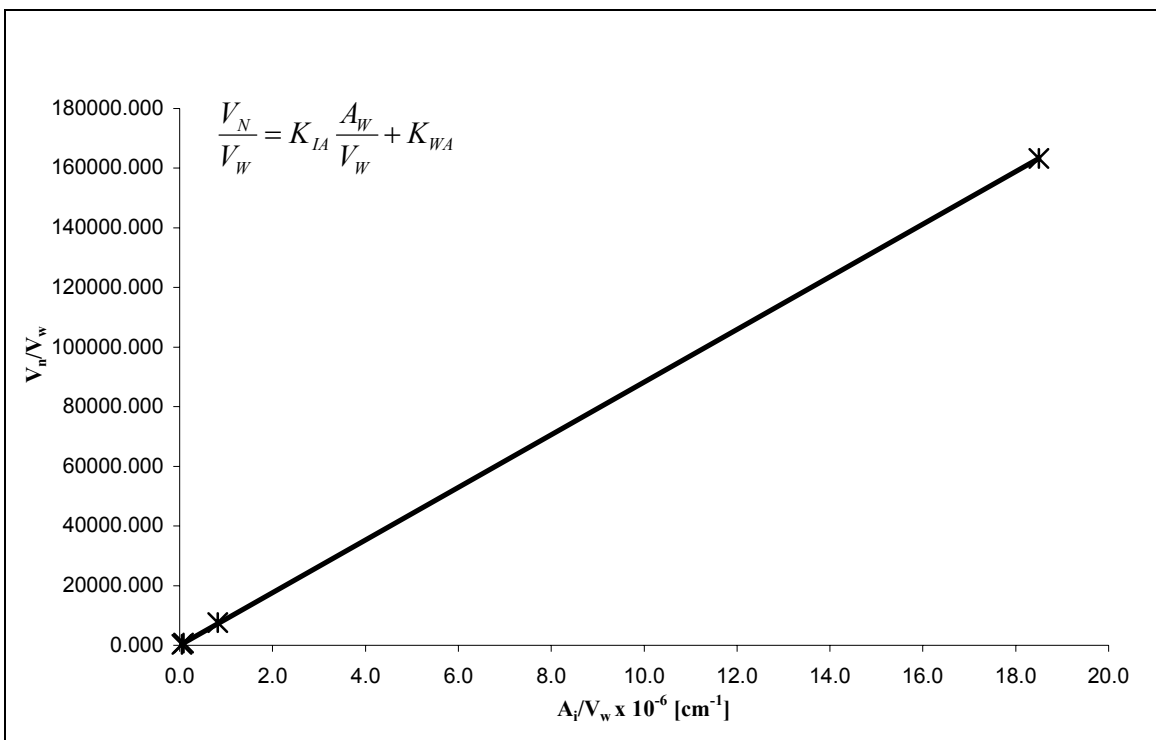


Figure19. Plot of V_N/V_W versus A_W/V_W for phenanthrene at 363 K ($R^2 = 0.99$).

The data obtained for phenanthrene at temperatures lower than 363 Kelvin resulted in a correlation coefficient that was lesser than the correlation coefficient for 363 Kelvin. The consequence for this lesser fidelity on lower temperature work with phenanthrene mostly owed to the innate chemical qualities of phenanthrene as an organic compound. However, the errors associated all the data in this work is consequently due to the difficulties in obtaining reproducible vapor samples at successive temperatures for each compound. Hence the K_{IA} obtained in this manner was extrapolated to room temperature, as it is almost impossible to obtain data on phenanthrene at room temperatures, was $1 \times 10^5 \mu\text{m}$. Table 6 shows the results for K_{IA} for phenanthrene at as function of temperature.

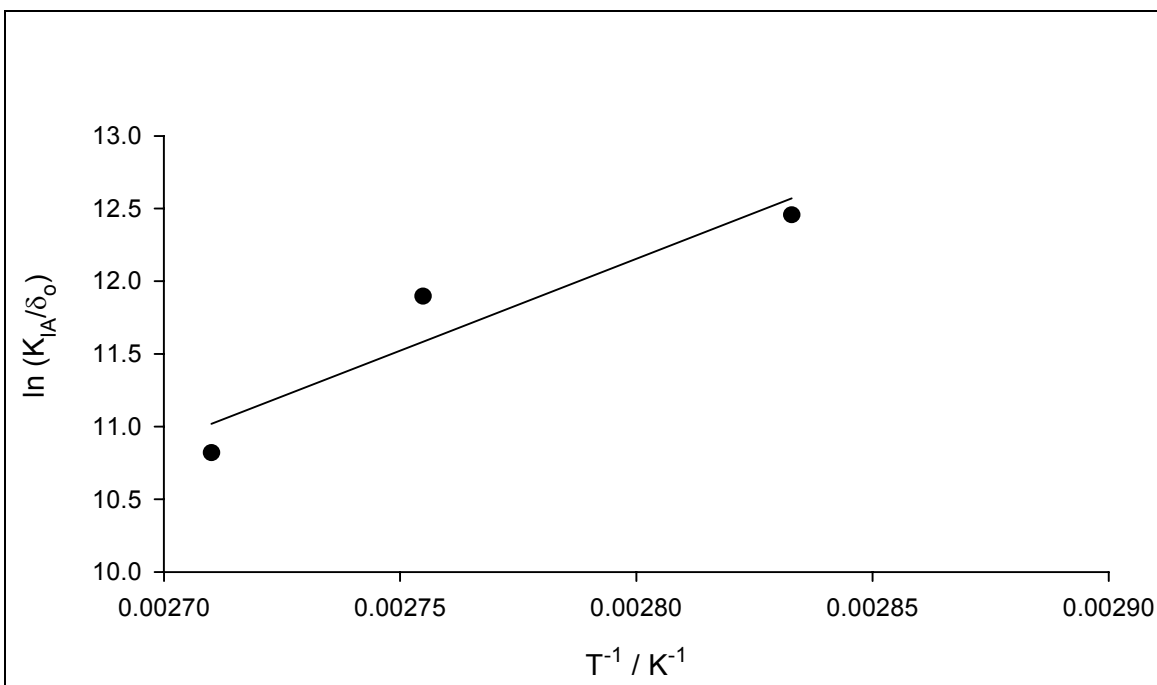


Figure 20. Integral form of the Gibbs-Helmholtz equation for phenanthrene ($R^2=0.892$).

Figure 20 shows the integral form of the Gibbs-Helmholtz equation for phenanthrene, which is used to obtain the heat of adsorption and the entropy of adsorption. The free energy of adsorption shown in Table 6 was calculated from the

$$\text{equation, } \Delta G_{IA}^0 = -RT \ln \left[\frac{K_{IA}}{\delta_0} \right].$$

TABLE 6. PHENANTHRENE PARTITION CONSTANT AS FUNCTION OF TEMPERATURE

Temperature (Kelvin)	K_{IA} (μm)	ΔG_{IA} (kJ/mol)
298	1×10^5	-47
353	156.31	-37
363	88.22	-36
369	4.18	-27

From the data in Table 6 for phenanthrene, we observe that similar trend in the result are observed as seen for naphthalene. Since phenanthrene is the more hydrophobic than benzene or naphthalene, K_{IA} is correspondingly very large. Also, for this larger molecule, phenanthrene, due to gain in entropy on de-sorption into the water and resulting in a more negative free energy, we can say that phenanthrene has lesser mobility than naphthalene or benzene. Also, the decreasing K_{IA} with temperature increase is an expected trend.

5.10 Analysis of Gas-Water Interface Adsorption Results

Table 7 shows the results that were obtained from the gas-water interface adsorption experiment for the three compounds considered in this work. The value of K_{IA} obtained from this work is in excellent agreement with other reported values. The data presented in this work are available at [Raja et al, 2002](#).

With the data obtained from adsorption experiments in gas-solid and gas-water interface, a comparison on the nature of the adsorbent is possible. The important properties that influence the adsorption process are the surface area and surface morphology of the adsorbent. The results shown for various water loadings clearly indicate the effect of surface area on adsorption.

The enthalpy of adsorption at the gas-solid interface is more negative than at the gas-water interface indicating that the adsorption is more favorable at the gas-solid interface. The enthalpy at the gas-solid interface being more negative also indicates the exothermic nature of the adsorption process on dry surfaces.

TABLE 7. PARAMETERS FOR ADSORPTION AT GAS-SOLID AND GAS-WATER INTERFACE

Property	Benzene	Naphthalene	Phenanthrene
Enthalpy of adsorption (ΔH_{SA}) [kJ/mol]	-45 ± 2 (this work)	-80 ± 2	-116.1 ± 0.3
Entropy of adsorption (ΔS_{SA}) [J/K·mol]	-73 ± 1 (this work)	-95 ± 5	-152 ± 5
K_{IA} (μm) at 298 K	0.43±0.01 (this work) 0.49 (Hoff et al, 1993) 0.41 (Braunt, 2000) 0.44 (Hoff et al, 1993)	27.2 ± 1.8	1×10^5 (extrapolated from high temperature)
ΔH_{IA} (kJ/mol)	-41 ± 2 (this work) -26 (Mmereki et al, 2000) -41 (Braunt, 2000) -31 (Suzuki et al, 1992) -31 (Dorris and Gray, 1981)	-67 ± 17	-104 ± 36
ΔS_{IA} (J/K·mol)	-82 ± 4 (this work) -83 (Braunt, 2000) -50 (Mmereki et al, 2000)	-135 ± 56	-195 ± 120
ΔG_{IA} (kJ/mol)	-16 ± 0.04 (this work)	-26.5 ± 0.01	-46 (extrapolated from high temp.)

5.10.1 Influence of Adsorbent Surface Morphology on Adsorbate Binding

The property, fractal dimension, that characterizes a surface morphology for various materials has been studied extensively and reported by [Anvir and Farin, 1984](#). This non-integer fractal dimension (D) is pertinent not only as a measure of surface irregularity, but also as a powerful quantitative tool for the study of surface structure and adsorbate-adsorbent interaction ([Pfeifer, 1983](#)). The adsorption characteristics of various adsorbents show a dependence of the fractal dimension on the adsorption. The value of D ranges from 2 to 3, where 2 represent a smooth planar surface and 3 represent a highly convoluted irregular surface. From the data reported ([Anvir and Farin, 1984](#)) for soil and other siliceous materials are about 2.92 and water surfaces are relatively smoother. [Gregg and Sing, 1982](#) cite observations for various adsorbents, where in smooth water has lesser adsorption than rougher surfaces. Hence, we can conclude that a smooth regular surface (D=2) offers lesser binding of the adsorbate to the adsorbent than a convoluted irregular surface (D=3). Thermodynamically speaking, the free energy value at the gas-solid interface is more negative than at the gas-water interface indicating that the adsorption is more favorable at the former interface, supporting the surface morphology theory. Also an irregular surface offers more mobility than a smooth regular surface ([Rigby and Gladden, 1999](#)). Conclusively, from the thermodynamic data, the entropy at the gas-water interface is distinctly more negative than at the gas-solid interface indicating greater mobility at the gas-solid interface.

5.10.2 Analysis of Interfacial Adsorption via Cluster Formation

From the discussion in the foregoing, we can assimilate that the adsorption of organic vapors is indeed a critical process and more critical for the hydrophobic compounds with regards to surface adsorption. The process of consideration now is to elucidate how the adsorbed vapor dissolves into the bulk liquid, and consequentially affect the prediction of gas-liquid partitioning as predicted by the Henry's Law.

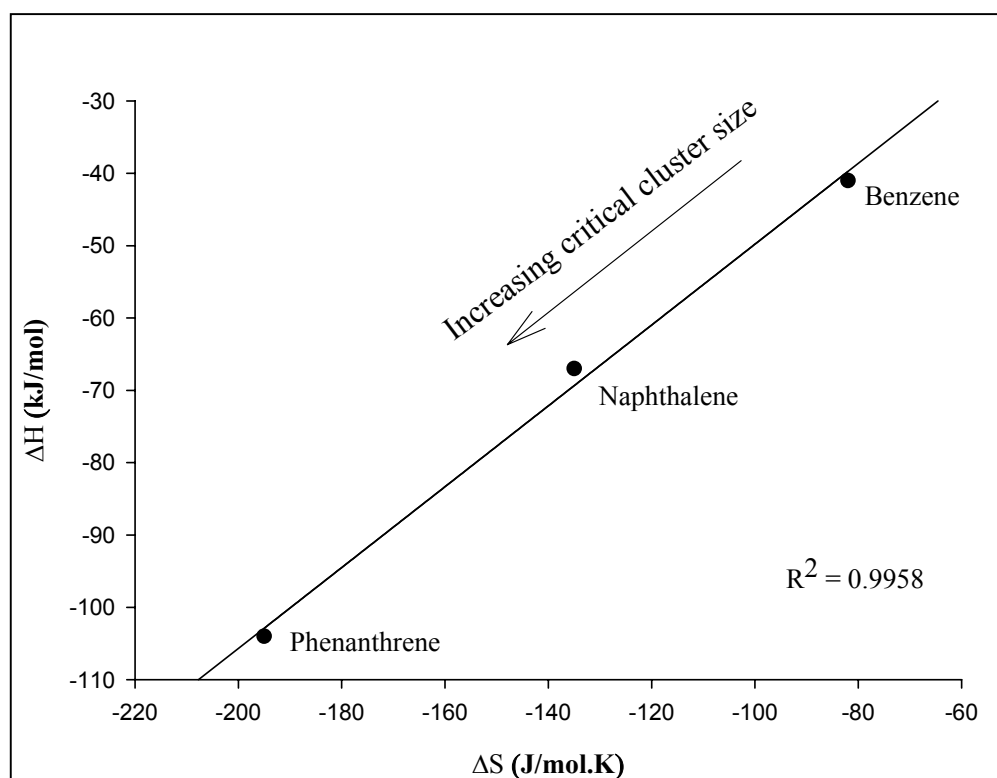


Figure 21. Critical cluster size for aromatic hydrocarbons from thermodynamic parameters.

The critical cluster model ([Nathanson et al, 1996](#)) described in the earlier chapter 2 defines that the gas-liquid transfer is a three-step model as, Adsorption \rightarrow Cluster Formation \rightarrow Solvation. The energy barrier illustrated in Figure 2 is overcome by formation of clusters and size of the cluster depends on the magnitude of this free energy

barrier. As the cluster reaches a critical size, it merges with the bulk liquid leading to dissolution of the gas phase species. Figure 21, shows a plot of the heat of adsorption versus entropy of adsorption at the gas-water interface. With increasing molecular weight, and decreasing vapor pressure, the critical cluster size required for subsequent dissolution is larger. Theoretically, we can expect the critical cluster size to be larger due to local structuring at the water surface for a hydrophobic molecule. Also, [Zhang et al, 2003](#) mention that the number of molecules required to form a cluster is lesser for molecules with larger attractive forces. We can observe that benzene, which is the most hydrophilic of the three, requires the least critical cluster size than phenanthrene.

[Davidovits et al, 1991](#) present equations for the entropy and enthalpy to determine the critical cluster size. Computation of the critical cluster size is not important in our context, but can be used to theorize the process of adsorption and dissolution at gas-liquid interfaces. However, the process surface adsorption and dissolution has been evidenced to support to the critical cluster model ([Nathanson et al, 1996](#)). Even our data tend to indicate support to this model.

The heat of condensation listed in Table 1 are less negative than the heat of adsorption for benzene, naphthalene, and phenanthrene at the gas-water interface. [Orem and Adamson, 1969](#) have observed similar trend for adsorption of organic vapors with low adsorption energies than heat of condensation at low surface coverage, and at high surface coverage the heat of adsorption was larger than the heat of condensation. The method of confirmation of adsorbate-adsorbent interaction by [Vidal-madjer et al, 1976](#) was by computing the adsorption potential for increasing number of layers of water surrounding the adsorbate molecule.

The larger enthalpy of adsorption than condensation has been explained to be because of the local structuring of water molecules around the organic molecules ([Orem and Adamson, 1969](#), and [Adamson, 1967](#)). Clearly, if the heat of adsorption is larger than the heat of condensation, it indicates stronger gas-water interactions than gas-to-gas interactions resulting in direct condensation. These observations support the critical cluster model in which the primary step is adsorption and sequential solvation. From these experimental results, it can be evidently seen that the transfer of gas into liquid is not limited to condensation of the gas species on the surface of the liquid, but rather involves the some kind of local structuring of the gas species resulting in adsorption and then ultimately solvation.

5.11 Correlation of K_{IA} and P_{SL}^0 for Aromatic Hydrocarbons

The partition constant K_{IA} obtained from this work is plotted together with results obtained for other aromatic hydrocarbons by ([Pankow, 1997](#)) are plotted in the Figure 22 as a function of the sub-cooled liquid vapor pressure P_{SL}^0 . Pankow obtained the values of K_{IA} for the sorption of PAHs and n-alkanes at the air/water interface by extrapolating solid gas partitioning data ([Storey et al, 1995](#)) to a 100% relative humidity. This extrapolated data is plotted together with the data obtained from this work show a good correlation ($R^2 = 0.9797$) for the compounds in this range of sub cooled liquid vapor pressure.

This correlation can be used to estimate K_{IA} values for those compounds for which the experimental partition constants are not as such available. However, this correlation is applies only to PAHs. The fact that our experimental values using the IGC technique are

in line with the estimates by [Pankow, 1997](#) who used a different methodology, is a proof that both methods are capable of obtaining accurate values of K_{IA} .

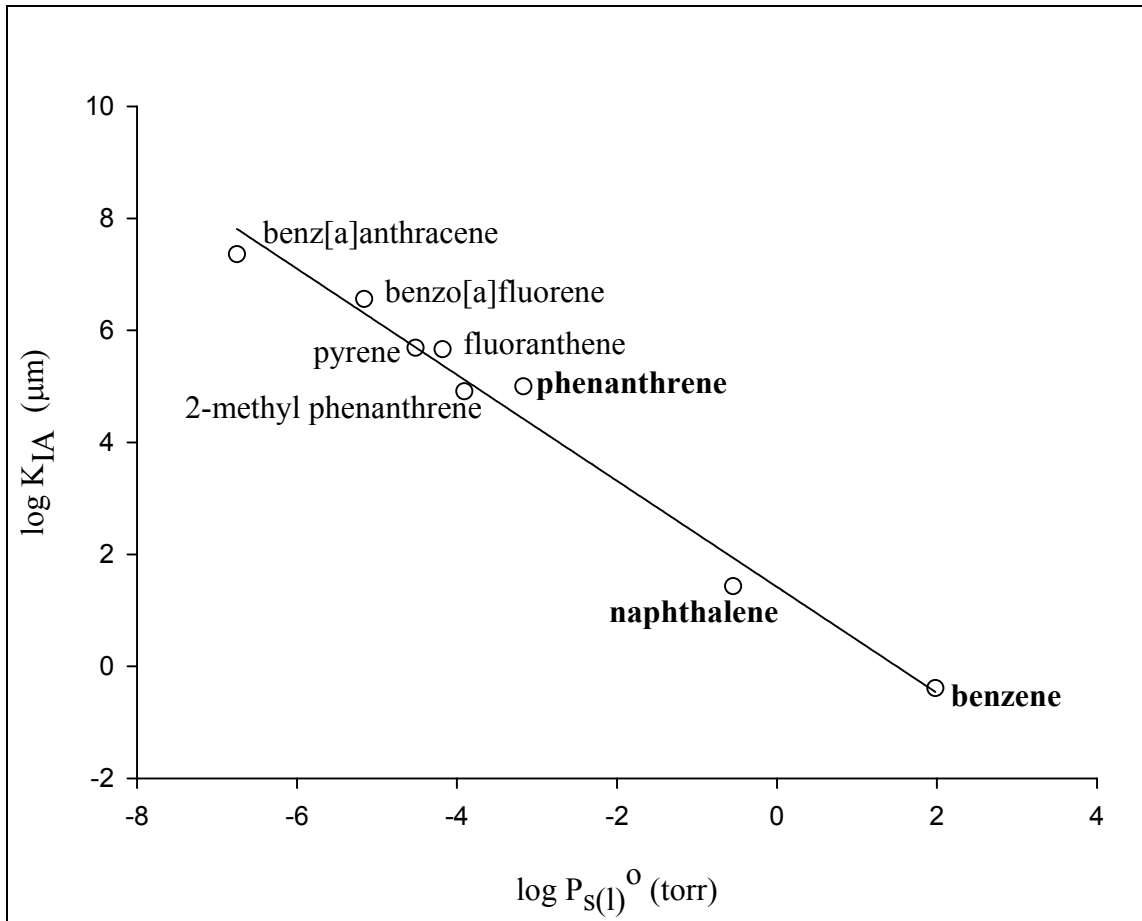


Figure 22. Correlation of $\log(K_{IA})$ and $\log(P_{SL}^0)$ for aromatic hydrocarbons. Data from this work and [Pankow, 1997](#). ($R^2=0.9797$).

CHAPTER 6

APPLICATIONS IN ATMOSPHERIC CHEMISTRY

6.1 Introduction

The earth's atmosphere is made of mostly gases with suspended solids and liquids. Atmospheric moisture, such as rain aerosol and fog-water, provides a reaction medium for pollutants. Fog droplets are generally in the size range of 1 and 10 μm with typical atmospheric lifetimes of a few hours ([Gill et al, 1983](#)). Fog formation is typically due to decrease in air temperature and an increase in relative humidity. As mentioned in various sections of these manuscripts, many researchers have observed very high concentrations of hydrophobic and pesticide compounds in the atmospheric moistures that were sampled. In this chapter, applications of the data determined and presented in the Chapter 5 will be discussed with relevance to atmospheric fate and transport of the chemical species.

6.2 Enrichment of Organic Vapors in Fog Water

[Valsaraj et al, 1993](#) have considered three important aspects for the enrichment of hydrophobic organics in fog water.

- (a) The importance of temperature correction for reported Henry's constants,
- (b) The effect of dissolved and colloidal organic material and other aqueous particles in fog water,
- (c) The effect of the large specific air-water interfacial area available for adsorption of hydrophobic organics.

There are several works that have explained the enrichment due to the presence of colloidal organic matter in the fog and cloud water ([Glotfelty et al, 1990](#), [Schomburg et](#)

[al, 1991](#), [Capel et al, 1990](#) and [Capiello et al, 2003](#)). From the data for K_{IA} in Table 4, 5 and 6 for benzene, naphthalene and phenanthrene indicate a negative trend with increasing temperature. Hence it can be evident that surface adsorption characteristics will change with temperature. However, the effect of temperature on Henry's constant has been studied extensively ([Snider and Dawson, 1985](#), [Gossett, 1987](#), [DeWulf et al., 1995](#), [Alaee et al., 1996](#), [Poddar and Sirkar, 1996](#)).

6.3 Transport of Gaseous Species into Fog Droplet

Consider a gas phase concentration C_g (mol/m^3) present around a droplet of fog water, and as a result the fog droplet experiences simultaneous dissolution and adsorption. From this, we can write that the total concentration of the liquid droplet (surface and bulk liquid) is

$$N_L (\text{mol}) = C_g (K_{IA}A_W + K_{WA}V_W) \quad (38)$$

In the above equation, C_g is the gas concentration, K_{IA} is the interface partition constant, A_W is the surface area of the water droplet, and K_{WA} is the dimensionless Henry's constant for bulk phase water-air partition constant and V_W is the volume of water in the fog droplet. This equation is similar to the IGC equation presented in equation (10), with surface adsorption and bulk dissolution term.

Equation (38) can be written as follows,

$$\frac{N_L (\text{mol})}{V_F (\text{m}^3)} = C_g \left(K_{IA} \frac{A_W}{V_F} + K_{WA} \right) = C_g \left(K_{IA} \frac{6}{d_p} + K_{WA} \right) \quad (39)$$

The surface adsorption concentration at the interface can also be written as follows from [Pankow, 1997](#).

$$C_{surf} (\text{mol} / \text{m}^2) = C_g \left(K_{IA} + \frac{h}{(H / RT)} \right) \quad (40)$$

From the “critical cluster model” it can be seen that the adsorbed organic vapor ultimately undergoes dissolution into the bulk liquid phase. A wet deposition with an ensemble of micron size droplets can lead to significant localization of the carcinogenic pollutant into a specifically confined area. The stomatal uptake from wet and dry deposition has received a lot attention with respect to pollution hazards not only from chemical and environmental engineers but also to botanists ([Geßler et al, 2002](#)).

TABLE 8. HENRY’S CONSTANT AND K_{IA} OF BENZENE, NAPHTHALENE AND PHENANTHRENE

Compound	K_{WA} [-] (Valsaraj, 2000)	K_{IA} (μm) (from this work)
Benzene	4	0.43
Naphthalene	50	27.2
Phenanthrene	697	1×10^5

The equation (39) can be rewritten as follows, for unit gas concentration and volume of fog water, to demonstrate the deviation in Henry’s law due to surface adsorption. In Equation (41), division of K_{WA} gives a normalized deviation in the Henry’s law constant, where d_p is the droplet diameter usually in the micron size range.

$$R_H = \frac{\left[K_{IA} \frac{6}{d_p} + K_{WA} \right]}{K_{WA}} \quad (41)$$

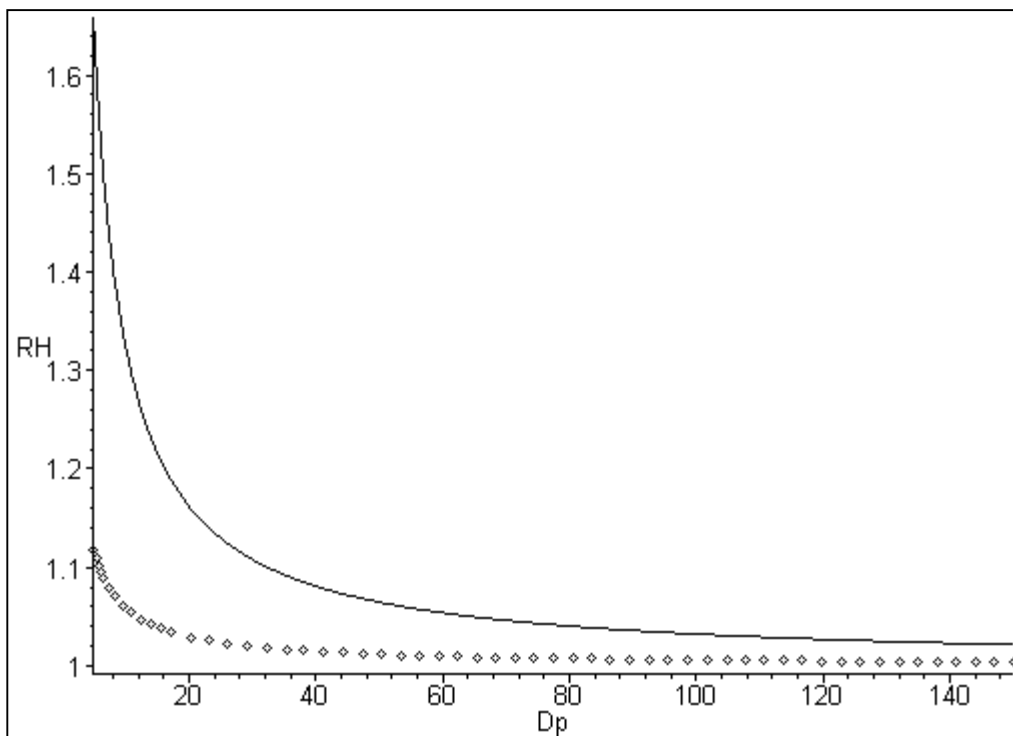


Figure 23. Normalized deviation in Henry's law versus droplet size in microns (Solid line - Naphthalene and Points - Benzene)

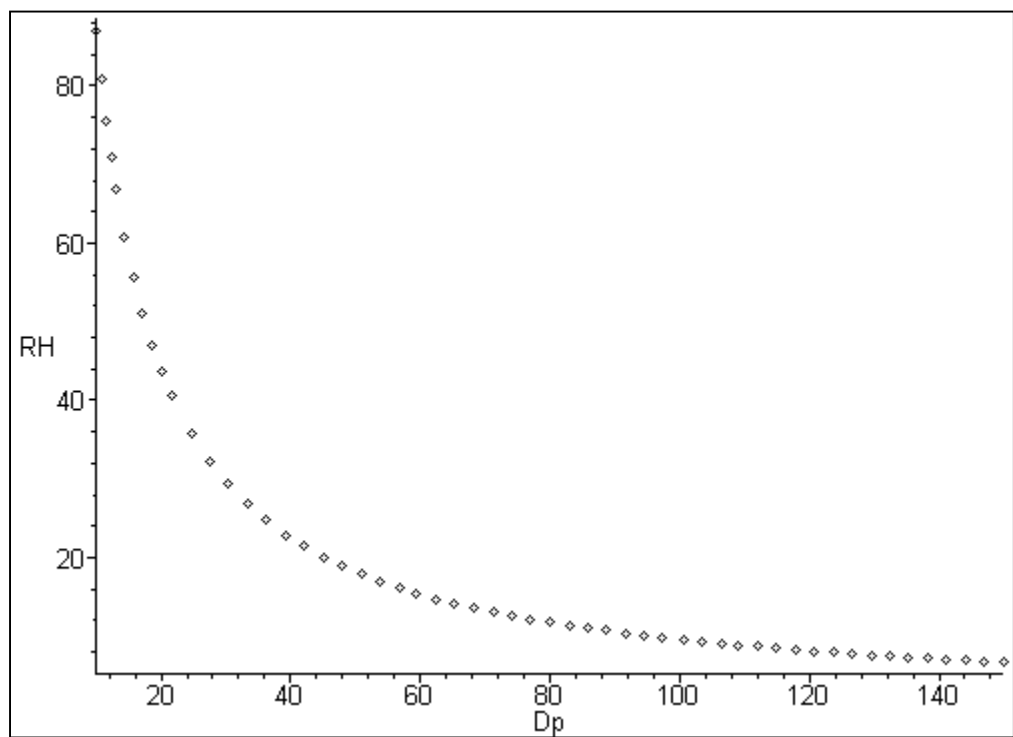


Figure 24. Normalized deviation in Henry's law versus droplet size in microns. (Phenanthrene)

From the Figure 21, deviation in Henry's law is about 1.12 for a 5 μ m droplet and approaches unity as the droplet size is increased. In the case of naphthalene, the normalized deviation approaches about 1.6 and is about two orders of magnitude higher for phenanthrene. The more hydrophobic the compound, larger is the deviation in Henry's constant, and its enrichment is far more greater than that predicted without surface adsorption. For molecules with large K_{IA} , the increased surface effects will become evident at smaller droplet sizes.

CHAPTER 7

CONCLUSIONS AND FUTURE WORK

7.1 Conclusions

The partition constant obtained for benzene in this work is in good agreement with data obtained by other workers. The correlation plot shows that the data obtained by the IGC technique is in line with the data of [Pankow, 1997](#) obtained from a different methodology. Hence, this is a proof that both methodologies can yield accurate values of K_{IA} . The importance of the droplet size in the scavenging efficiency is evident from this work. Hence, it would be an incorrect estimation of the overall concentration of the solute in the micron size droplet if the surface adsorption process were ignored. Hence, compounds with small K_{WA} and large K_{IA} will deviate considerably from the bulk phase Henry's law prediction. On the whole, the expected deviations in Henry's law will be smaller in the case of Benzene than for a more hydrophobic, high molecular weight, low vapor pressure compounds such as phenanthrene or pyrene.

7.2 Future Work

Experiments are currently being done to show the enrichment of micron size fog droplets in a laboratory environment and field sampling of fog water and air. The importance of surface adsorption process can be delineated clearly upon introduction various droplet sizes into the vapor phase compounds studied in this work. Also, molecular dynamics simulations are required to study the transport of vapor phase chemicals in to the aqueous phase.

REFERENCES

- Adamson, A.W., Dormant, L., and Orem, M., J., *Colloid Sci.*, 25, 206, (1967).
- Adamson, A.W., *Physical Chemistry of Surfaces* (4th Ed.), John Wiley and Sons, 1982.
- Alaee, M., Whittal, R.M., Strachan, W.M.J., The effect of water temperature and composition on Henry's law constant for various PAH's. *Chemosphere* 32 (6), 1153–1164, 1996.
- Andelman, J.B., and M.J. Suess (1970) Polynuclear aromatic hydrocarbons in the water environment. *Bull. Wld. Hlth. Org.* 43: 479-508.
- Andelman and Snodgrass (1972) Incidence and significance of polynuclear aromatic hydrocarbons in the water environment. *CRC crit. Rev. environ. Contr.* 4(1): 69-83.
- Avnir, D. and Farin, D., "Molecular fractal surfaces", *Letters to Nature*, 308, pp.261-263, 1984.
- Baek, S.O., Field, R.A, Goldstone, M.E., Kirk, P.W., Lester, J.N., and Perry, R. (1991) "A review of atmospheric polycyclic hydrocarbons: sources, fate and behavior, *Water. Air soil pollut.* 60, 279-300.
- Barrer, R.M., "Specificity in physical sorption", *Journal of colloid and interface science*", 21, 415-434, (1966).
- Bilinski, B., "The influence of thermal treatment of silica gel on surface-molecule interactions, II The gas phase titration", **201**, (1998), pp. 186-193.
- Bingham, E., Trosset R. P., Warshawsky D., "Carcinogenic potential of petroleum-hydrocarbons - critical-review of the literature", *Journal of environmental pathology and toxicology* 3 (1-2): 483-563 1979.
- Braunt, R. G., and Conklin, M. H. Dynamic Determination of Vapor Water Interface Adsorption for Volatile Hydrophobic Organic Compounds (VHOCs) Using Axisymmetric Drop Shape Analysis: Procedure and Analysis of Benzene Adsorption. *J. Phys. Chem. B* **2000**, 104, 11146-11152.
- Brunauer, Emmett and Teller, "Adsorption of gases in multimolecular layers", *Journal of american chemical society*, **60**, (1938), pp. 309-319.
- Cabani, S.; Gianni, P.; Mollica, V.; Lepori, L., "Group Contributions to the Thermodynamic Properties of Non-Ionic Organic Solutes in Dilute Aqueous Solution", *J. Solution Chem.* **1981**, 10, 563-595.

Capel, P.D., Gunde, R., Zunker, F., Giger, W., “Carbon speciation and surface tension of fog”, *Environmental Science and Technology* 24, 722-727, 1990.

Cappiello, A. et al, “Molecular Characterization of the Water-Soluble Organic Compounds in Fog-water by ESIMS/MS”, *Environmental Science and Technology*, 2003, 37, 1229-1240.

Cheng, W., Chu, F., Liou, J., “Air–water interface equilibrium partitioning coefficients of aromatic hydrocarbons”, *Atmospheric Environment* 37 (2003) 4807–4815.

Chiou, C. T.; Shoup, T. D. Soil Sorption of Organic Vapors and Effects of Humidity on Sorptive Mechanism and Capacity. *Environ. Sci. Technol.* **1985**, 19, 1196-1200.

Cruickshank, A.J.B., Windsor, M.L., and Young, C.L., *Proc. Roy. Soc., Ser. A* 295, 259 (1965).

Crutzen, P. J. and M. G. Lawrence, “The impact of precipitation scavenging on the transport of trace gases: A 3-dimensional model sensitivity study”, *J. Atmos. Chem.*, 37, 81-112, 2000.

Dang, L. X.; Feller, D. “Molecular Dynamics Study of Water-Benzene Interactions at the Liquid/Vapor Interface of Water”, *J. Phys. Chem. B* **2000**, 104, 4403-4407.

Davidovits, P., Jayne, J.T., Duan, S.X., Worsnop, D.R, Zahniser, M.S., Kolb, C.E., *J. Phys. Chem.*, 1991, 95, 6337.

Davies, J.T., Rideal, E.K., “Interfacial Phenomena (2nd edition)” Academic press, 1963.

De Seze, G. Sediments Air Partitioning of Hydrophobic Organic Chemicals. Ph.D. Dissertation, Louisiana State University, 1999.

DeWulf, J., Drijvers, D., van Langenhove, H., Measurement of Henry’s law constant as function of temperature and salinity for the low temperature range. *Atmospheric Environment* 29 (3), 323–331. 205–297, 1995.

Domingue, Joe; Burnett, Dan; Thielmann, Frank, “Using inverse gas chromatography (IGC) to investigate process-related changes in surface and bulk properties of pharmaceutical materials”, *American Laboratory* (Shelton, CT, United States) (2003), 35(14), 32-35, 37.

Dorris, G. M.; Gray, D. G. Adsorption of Hydrocarbons on Silica-Supported Water Surfaces. *J. Phys. Chem.* **1981**, 85, 3628-3635.

Dove, J. W.; Buckton, G.; Doherty, C., “A comparison of two contact angle measurement methods and inverse gas chromatography to assess the surface energies of theophylline and caffeine”, *International Journal of Pharmaceutics* (1996), 138(2), 199-206.

Eisenreich, S.J., Looney, B.B., Thornton, J.D., 1981. Airborne organic contaminants in the Great Lakes ecosystem. *Environmental Science and Technology* 15, 30–38.

Eley, D.D., *Trans. Faraday Soc.*, 35, 1281, 1939.

Facchini, M.C., Decesari, S., Mircea, M., Fuzzi, S., Loglio, G., “Surface tension of atmospheric wet aerosol and cloud/fog droplets in relation to their organic carbon content and chemical composition”, *Atmos. Environ.*, 34, pp. 4853-4857, 2000.

Franks, H.S., and Evans, M., *J. Chem. Phys.*, 13, 507, 1945.

Fuchs, N., “The mechanics of aerosols”, Pergamon press, New York, 1964.

Floris, F. M., Selmi, M., Tani, A., and Tomasi, J., *J. Chem. Phys.*, **107**, 6353, (1997).

Geßler, A., Rienks, M., and Rennenberg, H., “Stomatal uptake and cuticular adsorption contribute to dry deposition of NH₃ and NO₂ to needles of adult spruce (*Picea abies*) trees”, *New Phytologist*, (2002), 156, pp. 179–194.

Gill, P.S., Graedel, T.E., Weschler, C.J., “Organic films and atmospheric aerosol particles, fog droplets, cloud droplets, raindrops and snow lakes”, *Reviews of Geophysics and Space Physics*, 21, 903-920, 1983.

Glotfelty, D. E.; Seiber, J. N.; Liljedahl, L. A., “Pesticides in fog”, *Nature* (1987), 325(6105), 602-5.

Glotfelty, D. E.; Majewski, M. S.; Seiber, J. N., “Distribution of Several Organophosphorous Insecticides and their Oxygen Analogues in a Foggy Atmosphere”, *Environ. Sci. Technol.* **1990**, 24 (4), 353-357.

Goss, K. U. Adsorption of Organic Vapors on Polar Mineral Surfaces and on a Bulk Water Surface: Development of an Empirical Predictive Model. *Environ. Sci. Technol.* **1994**, 28, 640-645.

Goss, K.U., and Schwarzenbach, R.P., “Empirical prediction of heats of vaporization and heats of adsorption of organic compounds”, *Environ. Sci. Technol.*, 33, pp. 3390-3393, 1999.

Gossett, J.M., Measurement of Henry’s law constants for C1 and C2 chlorinated hydrocarbons. *Environmental Science and Technology* 21 (2), 202–208, 1987.

Gregg, S.J. and Sing, K.S.W., "Adsorption, Surface area, porosity", 2nd edition, New York, Academic Press, 1982.

Grimsey, Ian M.; Feeley, Jane C.; York, Peter, "Analysis of the surface energy of pharmaceutical powders by inverse gas chromatography", *Journal of Pharmaceutical Sciences* (2002), 91(2), 571-583.

Gustafsson, O.; Gschwend, P. M. Hydrophobic Organic Compound Partitioning from Bulk Water to the Water/Air Interface. *Atmos. Environ.* **1999** 33, 163-165.

Harkins and Brown, F.E., *J. Amer. Chem. Soc.*, 41, 499 (1919).

Hartkopf, A., Karger, B.L. *Acc. Chem. Res.*, 1973, 6, 209-216.

Hoff, J. T.; Mackay, D.; Gillham, R.; Shiu, W. Y. Partitioning of Organic Chemicals at the Air-Water Interface in Environmental Systems. *Environ. Sci. Technol.* **1993**, 27, 2174-2180.

Jenkins et al take from Barbara J. Finlayson Pitts

Karditsas, P., Taylor, J., "Polydisperse particulate transport modelling during a loca", *Fusion Engineering and Design* (2002), 63-64, 303-311.

Karger, B. L.; Castells, R. C.; Sewell, P. A.; Hartkopf, A. Study of the Adsorption of Insoluble and Sparingly Soluble Vapors at the Gas-Liquid Interface of Water by Gas Chromatography. *J. Phys. Chem.* **1971**, 75, 3870-3879.

Kemball, C.; Rideal, E. K., "The Adsorption of Vapors on Mercury. I. Non-Polar Compounds", *Proc. R. Soc. (London)* **1946**, A187, 53-73.

Kiselev, A.V., and Yashin, Y.I., "Gas-Adsorption chromatography", J.E.S. Bradley, trans., Plenum Press, New York, 1969.

Langmuir, I., *J. Amer. Chem. Soc.*, 40, 1361 (1918).

Lee, S.C., Ho, K.F., Chan, L.Y., Zielinska, B., Chow, J.C., "Polycyclic aromatic hydrocarbons (PAHs) and Carbonyl compounds in the urban atmosphere of Hong Kong", *Atmospheric Environment*, 35, (2001) 5949-5960.

Lewis, S. C.; King, R. W.; Cragg, S. T.; Hillman, D. W. Skin carcinogenic potential of petroleum hydrocarbons: crude oil, distillate fractions and chemical class subfractions. *Advances in Modern Environmental Toxicology* (1984), 6 (Appl. Toxicol. Pet. Hydrocarbons), 139-50.

Lum, Chandler and Weeks, "Hydrophobicity at Small and Large Length Scales", *J. Phys. Chem. B* **1999**, 103, 4570-4577.

Mackay, D., Shiu, W., Valsaraj, K.T., Thibodeaux, L.J., "Air-Water transfer: The role of partitioning", Air-Water Mass Transfer Second International Symposium U.S. Army Waterways Experiment Station/ASCE, Minneapolis, MN September 11-14, 1990.

McFarland, A. R.; Gong, H.; Muyschondt, A.; Wentz, W. B.; Anand, N. K., "Aerosol Deposition in Bends with Turbulent Flow", *Environmental Science and Technology* (1997), 31(12), 3371-3377.

Mmereki, B. T.; Hicks, J. M.; Donaldson, D. J. Adsorption of Atmospheric Gases at the Air-Water Interface. *J. Phys. Chem. A* **2000**, *104*, 10789-10793.

Munger et al, Fogwater Chemistry at Riverside, California, *Atmos. Environ.*, 24(B), 185-205, 1990.

Nathanson, G.M., Davidovits, P., Worsnop, D.R., and Kolb, C.E., "Dynamic and kinetics at the gas-liquid interface", *J. Phys. Chem.*, 100, pp. 13007-13020, 1996.

Neff, J. M., "Poly-cyclic Aromatic Hydrocarbons in the aquatic environment, sources fates and biological effects", Applied science publishers limited 1979.

Nikolaou, K., Masclet, P., and Mouvier, G. (1984) Sources and Chemical reactivity of polynuclear aromatic hydrocarbons in the atmosphere. A critical review, *Sci Total Environ.*, 32, 103-132.

Orem, M. W.; Adamson, A. W. Physical Adsorption of Vapor on Ice. II. n-Alkanes. *J. Colloid Interface Sci.* **1969**, *31*, 278-286.

Pandis, S.N., and Seinfeld, J.H., "Should bulk cloudwater and Fogwater samples obey Henry's Law?", *Journal of Geophysical research*, Vol. 96, No. D6, pp. 10,791-10,798, 1991.

Pankow, J.F., and Bidleman, T.F. (1991) "Effects of temperature, TSP and percent non-exchangeable material in determining the gas-particle partitioning in organic compounds", *Atmos. Environ.*, 24A, 2695-2698.

Pankow, J. F., "Partitioning of Semi-volatile Organic Compounds to the Air/Water Interface", *Atmos. Environ.*, 31, pp. 927-929, 1997.

Peters, J.A., Deangelis, D.G., and Hughes, T.W. (1981) in *Chemical Analysis and Biological Fate: Polynuclear Aromatic Hydrocarbons* edited by M. Cooke and A.J. Dennis Battelle press, Columbus, OH, pp. 571-582.

Pfiefer et al, "Chemistry in non-integer dimensions between two and three. I. Fractal theory of heterogeneous surfaces", *Journal of chemical physics*, **79**(7), (1983), pp. 3558-3565.

Poddar, T.K., Sirkar, K.K., Henry's law constants for selected volatile organic compounds in high-boiling oils. *Journal of Chemical and Engineering Data* 41 (6), 1329–1332, 1996.

Pohle, W. (1982) Infrared study of the adsorption of aromatic molecules onto silica and chlorinated silica, *Journal of chemical society, Faraday Transactions I.*, 78, 2101-2109.

Raja, S., "Simulation and benchmarking and aerosol transport in confined spaces", M.S. Thesis, Louisiana state University, 2001.

Raja, S., Yaconne, F.S., Ravikrishna, R., Valsaraj, K.T., "Thermodynamic Parameters for the Adsorption of Aromatic Hydrocarbon Vapors at the Gas-Water Interface", *J. Chem. Eng. Data* **2002**, 47, 1213-1219.

Ramdahl, T., Schjodager, J., Currei, L.A., Hanssen, J.E., Moller, M., Klouda, G.A., and Alfheim, I. (1984) Ambient impact of residential wood combustion in Elverum, Norway *Sci. Total Environ.*, 36, 81-90.

Reynolds S.T., Liu M.K., Hecht T.A., Roth P.M., Seinfeld J.H., "Mathematical modeling of photochemical air pollution--3. Evaluation of the model", *Atmospheric Environment* (1974 Jun), 8(6), 563-96.

Richards, L.W., et al, Hydrogen peroxide and sulfur (IV) in Los Angeles cloud water, *Atmos. Environ.*, 17, 911-914, 1983.

Sajo, E and Raja S, "A three-dimensional indoor aerosol transport model", *Health Physics*, 82 (6): S169-S170 Suppl. S JUN 2002.

Rigby, Sean P, Gladden, Lynn, "Molecular dynamics study on the mobility of Benzene and Water on silica surfaces: correlation with the influence of surface chemistry and morphology", *Studies in surface science and catalysis*, **122**, (1999), pp. 183-190.

Saxena, P.; Hildemann, L. M. Water-Soluble Organics in Atmospheric Particles: A Review of the Literature and Application of Thermodynamics to Identify Candidate Compounds. *J. Atmos. Chem.* 1996, 24, 57-109.

Schnelle-Kries, J. et al, "Occurrence of particle-associated polycyclic aromatic compounds in ambient air of the city of Munich", *Atmospheric Environment*, 35(1), 2001, S71-S81.

Schomburg, Charlotte J.; Glotfelty, Dwight E.; Seiber, James N., "Pesticide occurrence and distribution in fog collected near Monterey, California", *Environmental Science and Technology* (1991), 25(1), 155-60.

Schwartz, S.E., Mass transport considerations pertinent to aqueous phase reactions of gases in liquid water cloud water, *Atmos. Environ.*, 17, 911-914, 1983.

Seinfeld, J.H., Atmospheric Chemistry and Physics of Air Pollution, John Wiley, New York, 1986.

Seinfeld, J.H. and Pandis, S.N., "Atmospheric chemistry and physics - From air pollution to climate change", John Wiley and sons, inc., 1998.

Skoog, Holler and Newman, Principles of Instrumental Analysis, 5th edition, Harcourt Brace College Publishers, 1998.

Snider, J.R., Dawson, G.A., Tropospheric light alcohols, carbonyls, and acetonitrile: concentrations in the southwestern United States and Henry's law data. *Journal of Geophysical Research* 90 (D2), 3797-3805, 1985.

Storey, J.M.E., Luo, W., Isabelle, L.M., and Pankow, J.F., "Gas/solid partitioning of semivolatile organic compounds to model atmospheric solid surfaces as a function of relative humidity. 1. Clean quartz", *Environ. Sci. Technol.*, 29, 2420-2428.

Subramanyam, V.; Valsaraj, K. T.; Reible, D. D.; Thibodeaux, L., J., "Gas-to-Particle Partitioning of PAHs in an Urban Atmosphere", *Atmos. Environ.* **1994**, 28, 3083-3091.

Suzuki, S.; Green, P. G.; Bumgarner, R. E.; Dasgupta, S.; Goddard, A., III; Blake, G. A. Benzene Forms Hydrogen Bonds with Water. *Science* **1992**, 257, 942-945.

Valsaraj, K. T. On the Physicochemical Aspects of Partitioning of Nonpolar Hydrophobic Organics at the Air-Water Interface. *Chemosphere* **1988a**, 17, 857-887.

Valsaraj, K. T. Binding Constants for Non-Polar Hydrophobic Organics at the Air-Water Interface: Comparison of Experimental and Predicted Values. *Chemosphere* **1988b**, 17, 2049-2053.

Valsaraj, K.T., Thoma, G.J., Reible, D.D., and Thibodeaux, L.J., "On the enrichment of hydrophobic organic compounds in fog droplets", *Atmospheric Environment*, Vol. 27A, No. 2, pp. 203-210, 1993.

Valsaraj, K. T., "Elements of Environmental Engineering - Thermodynamics and Kinetics", 2nd ed.; CRC Press: Boca Raton, FL, 2000.

Van Ry, D., Gigliotti, C., Glenn IV, T., Nelson, E., Totten, L.A., Eisenreich, S.J., Vol. 36, No. 15, 2002, *Environmental Science & Technology*, pp.-3201

Vidal-Madjer, C.; Guiochon, G.; Karger, B. L. Adsorption Potential of Hydrocarbons at the Gas-Liquid Interface of Water. *J. Phys. Chem.* **1976**, 80, 394-402.

Weeks, J. D., Katsov, K., and Vollmayr, K., *Phys. Rev. Lett.* **81**, 4400, (1998).

Wilhelmy, Ann. Phys., 119, pp. 177, (1863).

Winiwarter, W et al, Organic acid gas and liquid measurements in Po valley fall-winter conditions in the presence of fog, *Tellus*, 40(B), 348-357, 1988.

York, P.; Ticehurst, M. D.; Osborn, J. C.; Roberts, R. J.; Rowe, R. C., "Characterization of the surface energetics of milled dl-propranolol hydrochloride using inverse gas chromatography and molecular modeling", *International Journal of Pharmaceutics* (1998), 174(1-2), 179-186.

Zappoli, S.; Andracchio, A.; Fuzzi, S.; Facchini, M. C.; Gelencsér, A.; Kiss, G.; Krivásky, Z.; Molnár, A.; Mezős, E.; Hansson, H. C.; Rosman, K.; Zebühr, Y. *Atmos. Environ.* **1999**, 33, 2733-2743.

Zhang, H.Z., Li, Q., Y., Xia, J.R., Davidovits, P., Williams, L.R., Jayne, J.T., Kolb, C.E., and Worsnop, D.R., "Uptake of gas-phase species by 1-octanol. 1. Uptake of α -pinene, γ -terpinene, p-cymene, and 2-methyl-2hexanol as function of relative humidity and temperature", *J. Phys. Chem. A*, 107, 6388-6397, 2003.

Zhang, Q., Anastasio, C., "Chemistry of fog waters in California's Central Valley Part 3: concentrations and speciation of organic and inorganic nitrogen", *Atmospheric Environment* 35 (2001) 5629–5643.

VITA

Suresh Raja graduated from Boston Matriculation Senior Secondary School, Madras, India in 1994. He then attended University of Madras from 1994 to 1998 to earn a bachelor's degree in Chemical Engineering. In fall 1998, he was the recipient of the graduate school award at American University, Washington, D.C. He came to the LSU graduate school in 1999 to earn a master's degree in physics and continued graduate studies in chemical engineering to earn a master's degree. He will continue studies to earn a doctoral degree. He is currently a master's candidate in the department of chemical engineering.